Seedlings of Temperate Tree Species Show Plastic Responses to Water Deficit and Heat Stress, But They Do Not Prevent Decline in Growth

Lina Aragón[1,2], Christian Messier[2] and Julie Messier[3,4]

[1] Department of Biology, University of Miami, Coral Gables, FL 33146, USA
[2] Department of Biology, University of Waterloo, Waterloo, Ontario, Canada
[3] Centre d'Étude de la Forêt, Université du Québec à Montréal, Montréal, QC, Canada
[4] Institut des Sciences de la Forêt Tempérée, Université du Québec en Outaouais, Ripon, QC, Canada

Abstract

Species response to climate change is difficult to predict because warming involves the interaction of multiple stressors whose effects are simultaneous and therefore difficult to disentangle. To address this gap, I studied the effect of global warming on plant performance and functional traits by exposing seedlings from five temperate tree species with distinct life histories to water deficit and heat individually and combined. I evaluated for each species: 1) the performance response, and 2) the multivariate phenotypic plastic response to water deficit and heat individually and combined, and 3) how functional traits mediate the tree's performance response to those stresses.

In a greenhouse, 180 individuals grown in pots from *Acer saccharum, Betula alleghaniensis, Quercus rubra, Picea glauca,* and *Pinus resinosa* were exposed to six treatments using a fully crossed factorial design with three water deficit levels (low: 38.2%, medium: 35.7%, and high: 31.3%) and two temperatures (ambient temperature and warmer temperature: +0.42°C). To have a holistic understanding of the species response, I studied a total of 33 functional traits from the leaf (26), stem (2), and roots (5) related to various vital ecophysiological functions.

We found that future warmer and drier conditions will decrease plant performance and impact different species differently. The seedlings' performance response was stronger to water deficit than heat, while their plastic trait response was stronger to heat than water deficit. These results highlight that performance and phenotypic responses can be sensitive to different environmental factors. Further, in each species, different traits responded to these two environmental stressors, indicating that the effects of global warming on the phenotype will differ among species. Although heat will lead to water deficit via increased evaporation, results showed that heat and water deficit in all species impact different sets of functional traits. Phenotypic response to global warming sits at the intersection of these two responses, making them more complex to assess. Last, only a total of five traits from three different species contributed to maintaining plant performance under water deficit conditions. Still, performance drastically declined in these species, indicating that those plastic responses were insufficient to offset the effect of stressful environmental conditions.

Introduction

Temperate forests in Canada will experience higher summer temperatures with similar precipitation due to global warming (Cohen et al., 2019). This combination of environmental conditions leads to a higher vapor pressure deficit coupled with higher evapotranspiration demands decreasing water availability (Stéfanon et al., 2014). Plant species from this ecosystem should be capable of responding to these changes by showing changes in their anatomical, morphological, and physiological traits that will allow them to maintain their performance under more stressful environmental conditions (Aitken et al., 2008; Sultan, 2004). In this study, we aim to understand the plastic response of five Canadian tree species to water deficit and heat individually and combined under controlled environmental conditions.

Canada was warmed during the last century and will warm further (Cohen et al., 2019). In southern Canada, the mean annual temperature increased by 1.9°C between 1900 and 2016, with increases by 1.3°C and 1.1°C in Ontario and Quebec, respectively (Cohen et al., 2019). Moreover, in southern, eastern Canada (Ontario and Quebec regions), temperatures are predicted to warm by 1.5°C between 2031 - 2050, with longer and warmer summers and more variable precipitation (Cohen et al., 2019). Precipitation has increased from 1948 to 2012, and in southern Canada is expected to show a slight increase (10%) under a low emission scenario while a slight decrease (10%) under a high emission scenario (Zhang et al., 2019). Temperate forests in Canada comprise 9% of the world's total forest cover (346 million ha) and have suffered from climate-driven tree mortality due to drought and heat stress (Allen et al., 2010; FAO, 2020; van Mantgem et al., 2009). These predictions and the observed effects of warmer and drier conditions make it imperative to understand the interactive effects of water deficit and heat on plant species' performance.

Species can avoid extinction under global warming conditions by shifting their geographical distribution to track optimum environmental conditions, adapting to new environmental conditions through genetic variations, and acclimatizing to tolerate the new conditions through plastic changes in their phenotype (Aitken et al., 2008; Feeley et al., 2012). Of these three non-exclusive options, phenotypic plasticity has been shown to be relevant in the short term by providing species with a buffer response against rapid and unexpected changes in climatic conditions (Bonamour et al., 2019). In the narrow sense, phenotypic plasticity is defined as a genotype's ability to express different anatomical, morphological and physiological trait values under different environmental conditions (Pfennig & Jane West-Eberhard, 2021). Some of the limitations to studying narrow sense phenotypic plasticity is that thousands of individuals of several genotypes from different populations are required (Pigliucci, 2003). Thus, I studied phenotypic plasticity broadly by assessing for a given species how much and in which direction functional trait values change under different environmental conditions.

Functional traits mediate an organism's functional response to environmental conditions providing us with the tools to test the effects of global warming on species' functioning (Heilmeier, 2019). Functional traits are anatomical, morphological, and physiological attributes that affect an individual's performance (i.e., growth, reproduction, and survival), indirectly affecting their fitness (Violle et al., 2007). Trait plasticity is only adaptive when the change is in the right amount and speed, optimizing growth, survival and reproduction (Maire et al., 2013; Sultan, 2004; Walters & Gerlach, 2013). Trait-based ecology has successfully quantified species-level interactions among functional traits, plant performance, and environmental gradients (e.g., leaf economics spectrum (I. J. Wright et al., 2004), wood economics spectrum (Chave et al., 2009), root economic spectrum: (Weemstra et al., 2016), and whole plant economic spectrum (Reich, 2014)). Still, the question remains about how functional traits will mediate the within species' performance response to climate change and what mechanisms will be involved in this process (Sultan, 2004).

Species response to climate change is difficult to predict because warming involves the interaction of multiple stressors whose effects are simultaneous and therefore difficult to disentangle. This study contributes to further our understanding of the possible responses of species to future global warming by exposing seedlings from five temperate tree species with distinct life histories to water deficit and heat individually and combined. In a greenhouse, 180 seedlings from *Acer saccharum*, *Betula alleghaniensis*, *Quercus rubra*, *Picea glauca*, and *P. resinosa* were exposed to three water deficit levels (low, medium, and high) and two temperatures (ambient and warmer temperatures) using a fully crossed factorial design.

Based on the direct and indirect effects of environmental conditions on plant species performance (Figure 1), I first evaluated the species performance response by answering what water deficit and heat's individual and combined effects on plants' relative growth rate are (Figure 1., blue arrow). Then, I evaluated the species' multivariate phenotypic responses by answering which functional traits respond to water deficit individually and combined (Trait ~ Environment) and how much and in which direction they change (ΔTrait ~ Environment) (Figure 1., green arrow). Last, I evaluated how functional traits mediate the tree's performance response (RGR) to water deficit and heat by identifying which traits contributed to maintain performance under stressful environmental conditions (ΔPerformance ~ ΔTraits) and if the same plastic traits across species mediate their performance responses (Figure 1, purple arrow).

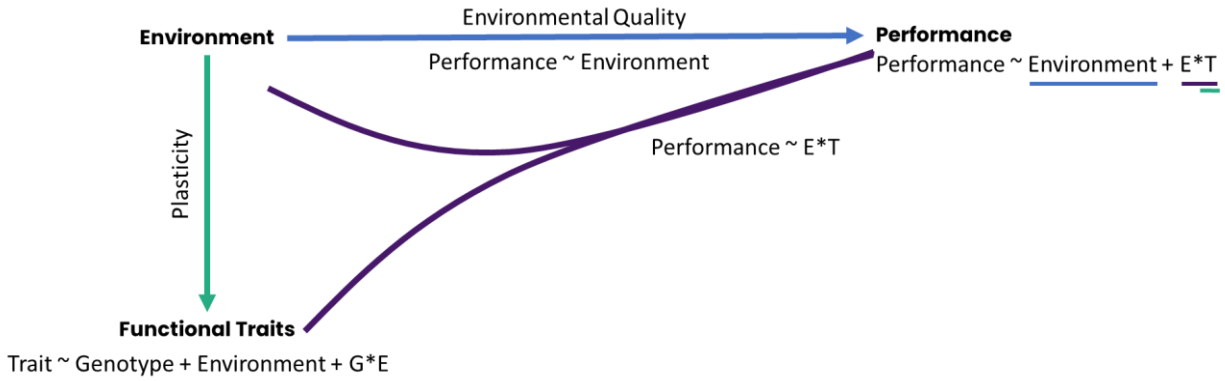

Figure 1. Graphical representation of the relationship among the environment, functional traits, and performance.

Methodology

Experimental Design

In a greenhouse five tree species were exposed to six different environments by using a factorial design of three water levels: low-water deficit (LWD), medium-water deficit (MWD), and high-water deficit (HWD), and two temperatures: ambient temperature: without open-top chamber (w/o OTC) and warmer temperature with an open-top chamber (OTC). The six treatments will be represented as follows: LWD without OTC: L-, LWD with OTC: L+, MWD without OTC: M-, MWD with OTC: M+, HWD without OCT: H-, and HWD with OTC: H+. Trees were set on ten tables total and rotated twice a week to account for variation in temperatures within the greenhouse. I blocked the experiment by assigning five tables to each of the two temperatures. Each table had 18 trees with three individuals per species, each in one of the three water levels and three additional individuals of one species in each of the water levels. Therefore, I had six treatments x five species x six replicates for 180 trees. The position of the individual trees in each table was randomized, and I rotated the tables biweekly on Tuesday and Friday mornings. The experiment ran from June 1st to September 20th, 2021.

I conducted this experiment in the greenhouse at the University of Waterloo (Waterloo, ON, Canada) using five native Canadian tree species commonly used in forestry: *Acer saccharum* (ACSA), *Betula alleghaniensis* (BEAL), *Picea glauca* (PIGL), *Pinus resinosa* (PIRE), and *Quercus rubra* (QURU). Saplings between two and three years old were obtained as tube stock from the Pépinière et centre de semences forestières de Berthier, Ministère des Forêts, de la Faune et des Parcs (1690, Grande-Côte Berthier (Québec), J0K 1A0). Saplings were transplanted into circular pots (height: 17 cm, diameter: 20.32cm, volume: 3.8L) containing a potting mix (80% Canadian sphagnum peat moss: 20% coarse perlite, ASB Greenworld, 332911 Plank Line, Mount Elgin, ON N0J 1N0). The trees grew and acclimated to each change in conditions for one week. I first put all the trees in LWD for a week; then, I moved the trees assigned to the MWD and HWD to the MWD treatment for another week; and finally, the trees assigned to HWD were moved to this treatment.

I created the three water deficit levels using the "Snow and Tinger system" (Fernández & Reynolds, 2000; Marchin et al., 2020; Snow & Tingey, 1985). This system uses capillarity irrigation to control the pots' soil water content. Therefore, the "Snow and Tinger system" maintains a constant water potential in the pots to assess a species' response to a fixed level of water availability because all plants experience a standard water deficit irrespective of their overall size, and root size or properties (Fernández & Reynolds, 2000; Lambrecht et al., 2007; Marchin et al., 2020). Potted plants are placed on top of a solid column of material with low water permeability (here, floral foam: 22.4 cm x 7.6 cm x 10.4 cm) located inside a bucket filled with water maintained at a constant level (Figure 2). Water moves from the bucket to the soil by capillary action, such that the taller the water column, the larger the distance between the bottom of the potted plants and the water table, stronger the intensity of the water deficit (i.e., 0 – 5 cm: low water deficit, 5 – 15 cm: medium water deficit, 20 – 25 cm: high water deficit) (Fernández & Gyenge, 2010). Based on a pilot project ran during the summer of 2020, I used the following three levels: 2.4 cm for LWD, 12.8 cm for MWD, and 23.2 cm for HWD (Figure 2).

I used open-top chambers (OTC) built to fit around individual trees to elevate the air and soil temperatures. OTC is a simple, cost-effective solution to simulate warming climate conditions in the field and controlled experiments with many replicates (Welshofer et al., 2017). They are small hexagonal or cylindrical greenhouse chambers made of translucent Plexiglas without UV protective coating that allows high solar transmittance and natural ultraviolent conditions (de Frenne et al., 2010; Welshofer et al., 2017). Therefore, OTC passively warms the inside air and soil by capturing the soil radiation allowing natural light levels and gas exchange (de Frenne et al., 2010). I used cylindrical chambers constructed from 2-mm-thick, UV-transmissive plexiglass, with a 13 cm hole in the lid to prevent warm air escape (Figure 2).

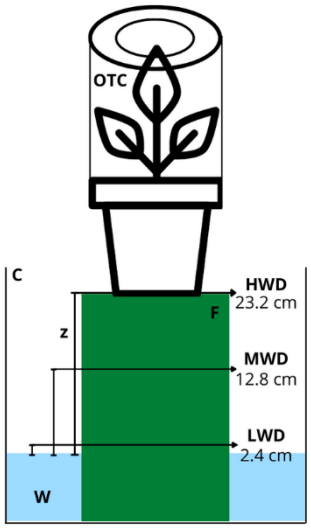

Figure 2. Diagram of the water deficit method, including the open-top chamber (OTC) to increase the air and soil temperature. The distance (z) between the water table (W) and the top of

the solid column of low water permeability (F) determines the degree of water deficit (LWD: low water deficit, MDW: medium water deficit, HWD: high water deficit) (Adapted from Marchin et al. (2020)).

Environmental conditions

I measured the environmental conditions imposed on the plants by using 90 Flower Care™ sensors assigned to three OTC tables and two w/o OTC tables. The sensors recorded the Air Temperature (°C, AirTemp) and Soil Humidity (%, SH) every hour during the experiment. Additionally, I used a Teros 12 Soil Moisture Sensor to measure the volumetric water content (m^3/m^3, VWC), temperature (°C, SoilTemp), and bulk density (dS/m, BD) of each of the pots at least once per month.

Functional Traits

To assess the response of trees to water deficit and warming, I measured functional traits from the leaves, stem, roots, and the whole plant, reflecting a set of key physiological functions (Table 1.). I focused on assessing those physiological functions expected to be affected by water deficit and heat that also could play a role in maintaining plant performance under these stresses. These are photosynthesis, water use, water transport, carbon assimilation, photoprotection, and thermoregulation. Other key functions assessed are nutrient and water acquisition.

Table 1. Traits measured, abbreviations, units, and associated physiological function: resource acquisition (RA), resource conservation (RC), water transport: (WT), temperature regulation (TR), photoprotection (PP), mechanical support (MS), resource storage (RS), biomass allocation (BA).

Traits	Abbr.	Units	Putative functional role
Leaf traits			
Stomatal density	SD	mm^{-2}	RA – WT
Stomatal size	SS	μm	RA – WT
Stomatal Pore Index	SPI	%	RA – WT
Leaf thickness	LT	mm	RA – WT
Leaf mass per area	LMA	$g\ m^{-2}$	RA – WT
Leaf water potential at turgor loss point	ψ_{TLP}	MPa	RA – WT
Osmotic potential at full turgor	ψ_{100}	MPa	RA – WT
Relative water content at turgor loss point	RWC_{TLP}	%	RA – WT
Modulus of elasticity	ε	%	RA – WT
Predawn water potential	ψ_{PD}	MPa	RA – WT
Midday water potential	ψ_{MD}	MPa	RA – WT
Delta water potential	$\Delta\psi$	MPa	RA – RC –

			WT
Leaf temperature differential	LTD	°C	TR
Linear electron flow	LEF	unitless	RA
Non-photochemical quenching estimated	NPQt	unitless	PP
Quantum Yield of Photosystem II	Phi2	unitless	RA
Ratio of incoming light that goes towards non-photochemical quenching	PhiNPQ	unitless	PP
Ratio of incoming light lost via non-regulated processes	PhiNO	unitless	PP
Relative chlorophyll concentration	CHL	mg m^{-2}	RA
Maximum carbon assimilation per area	A_{MAX}^{A}	µmol CO_2 m^{-2} s^{-1}	RA
Maximum carbon assimilation per mass	A_{MAX}^{M}	µmol CO_2 g^{-1} s^{-1}	RA
Stomatal conductance	g_s	mol H_2O m^{-2} s^{-1}	RA
Transpiration rate	E	mmol H_2O m^{-2} s^{-1}	RA – TR
Instantaneous water use efficiency	WUE	µmol CO_2 $mmol^{-1}$ H_2O	WT
Intrinsic water use efficiency	WUEi	µmol CO_2 mol^{-1} H_2O	WT
Leaf carbon isotope concentration	$\delta^{13}C$	VPDB ± 0.2‰	WT
Stem traits			
Hubber value	HV	m^2 m^{-2}	WT – BA
Stem specific density	SSD	g cm^{-3}	WT – MS – RS
Root Traits			
Root dry matter content	RDMC	g g^{-1}	RC
Specific root length	SRL	m g^{-1}	RA
Average root diameter	ARD	mm	RA
Biomass Allocation			
Leaf mass fraction	LMF	g g^{-1}	RC – BA
Root mass fraction	RMF	g g^{-1}	RC – BA

Leaf traits

At the leaf level, I studied 26 anatomical, morphological, and physiological traits related to carbon, water, and light use (Table 1).

Anatomical traits like the stomata density and size regulate plant water loss. Leaf prints from the adaxial and abaxial surfaces were taken using transparent nail polish for the broadleaf species. The polish was peeled off the leaf and put on a slide for further inspection under the microscope. All the broadleaves' species were classified as hypostomatic, meaning they only have stomata on the abaxial surface of the leaf. I took three photos of different locations from each abaxial

surface of each leaf at 40x magnification, and three leaves per individual were used for this process. Stomata were counted and measured on each photo using Fiji. Stomatal density (SD, μm^{-2}) was measured as the average number of stomata per unit area for the three leaves studied per individual. The stomatal length (SL, μm) and width (SW, μm) were obtained from three randomly selected stomata per photo. The stomata pore index (SPI, %) is an integrative trait based on both stomatal density and size that reflects the leaf stomatal conductance. SPI was calculated as:

$$SPI = stomatal\ density \times stomatal\ length^2 \times 10^{-4} \quad \textit{Eq. 1}$$

Morphological traits have been found to be related to the plant's photosynthetic capacity, resource-use strategy, environment affinity, and water transport (I. J. Wright et al., 2004). We studied the leaf mass per area (LMA, g m^{-2}), leaf area (LA, m^{-2}), and leaf thickness (LT, mm) as morphological traits.

Physiological traits were studied to determine the individual use of water, carbon, and light to photosynthesize, maintain water transport, and avoid photoinhibition and heat stress. All these traits were measured after two months of the experiment during the week of August 9 – 13, 2021. Every day two tables, one per block, were measured.

The individuals' capacity to regulate their hydric status was studied by measuring water potential twice a day (Williams & Araujo, 2002). Predawn water potential (ψ_{PD}, MPa – 3:00 – 5:00 h) represents the point where the plant is under its best hydric status, and the 'leaves' water potential is almost equal to the soil water potential. Midday water potential (ψ_{MD}, MPa – 12:00 – 14:00 h) represents the worst hydric status of the plant due to tremendous evaporative water demand (Choat et al., 2012). The daily change in water potential ($\Delta\psi = \psi_{MD} - \psi_{PD}$, MPa) has been related to the plant's ability to regulate water gains and losses. Water potential measurements were done using a Scholander Pressure Chamber (Model 1505D-EXP/PMS- Instrument- Albany, OR). One leaf per individual was used for the predawn and midday measurements in broadleaves, and the leaf used for the gas-exchange measurements was the same used to take the midday water potential. For the conifers, three needles per individual were used both at predawn and midday and the water potential values reported are the average of those three needles.

To find the light intensity (PAR) at which the maximum carbon assimilation was achieved for each species, I performed light response curves in the two most contrasting treatments of the experimental design: with neither stress (L-) and with both stresses (H+). Before the week of measurements, light curves were performed using a LiCor 6800 (Li-Cor, Lincoln, NE, USA). The instrument automatically ran the curve, and 11 photon flux densities (μmol m^{-2} s^{-1}) were used: 2500, 2000, 1500, 2500,1250, 1000, 500, 250, 100, 50, and 0. Each photon flux density was maintained for 5 minutes. I fitted each light response curve to the eleven models proposed by Lobo et al. (2013), and the curve with the smallest sum of square errors was selected as the

best-fitted curve. I found that for all species, the light saturation point was below 1000 µmol m^{-2} s^{-1}, so I used 1500 µmol m^{-2} s^{-1} to get the maximum carbon assimilation in a shorter period of time. I then performed acclimatization curves in which a leaf was exposed to 1500 µmol m^{-2} s^{-1} for an hour, and photosynthesis was recorded every 2 minutes to determine the percentage of the maximum photosynthesis a leaf could achieve if the measurement was taken after only 5 minutes. I found that after 5 minutes, the value of carbon assimilation taken represented for *A. saccharum:* 68.9%, *B. alleghaniensis:* 74.4%, *P. resinosa:* 89%, and *Q. rubra:* 63.2% of the maximum carbon assimilation. This procedure was not done for *P. glauca* due to the limitations of the chamber design to fit these needles. I proceeded with all future photosynthesis measurements after 5 minutes of acclimation to 1500 µmol m^{-2} s^{-1}.

During the week of measurements, carbon assimilation was measured from 10:00 to 12:00 in a young, fully developed leaf. I set the light to 1500 µmol m^{-2} s^{-1}, the CO_2 to 400 ppm, the stomatal ratio to 0 for the broadleaves, and 0.5 for the conifers and took the measurements after 5-min of acclimatization. From these measurements, I obtained maximum carbon assimilation per area (A_{MAX}^{A}, µmol CO_2 m^{-2} s^{-1}) and per mass (A_{MAX}^{M}, µmol CO_2 g^{-1} s^{-1}), transpiration rate (E, mmol H_2O m^{-2} s^{-1}), stomatal conductance (gs, mol H_2O m^{-2} s^{-1}), instantaneous water-use efficiency (insWUE, µmol CO_2 $mmol^{-1}$ H_2O), and intrinsic water use efficiency (intWUE, µmol CO_2 mol^{-1} H_2O).

Chlorophyll is the pigment that mainly drives photosynthesis. The concentration of this pigment can be affected by stressful environmental conditions being a proxy of the plant's state. We measured the chlorophyll concentration (CHL, mg m^{-2}) using a chlorophyll content meter capable of handling small needless (CCM-300, Opti-Sciences, Hudson, USA).

Light absorbed by the photosynthetic apparatus has three competing fates (photochemistry, heat dissipation, chlorophyll fluorescence) that can show responses to environmental changes. I assessed the status of the photosynthetic apparatus by taking chlorophyll fluorescence measurements with the MultispeQ v2.0 controlled by the PhotosynQ platform. The MultispeQ v2.0 measured the leaf relative chlorophyll content, the quantum yield of photosystem II that measures the amount of energy used toward photosynthesis (Phi2 – photochemistry), and the ratio of incoming light that goes towards non-photochemical quenching that measures the amount of energy that is dissipated as Heat (PhiNPQ – heat dissipation), and the ratio of incoming light that is lost via non-regulated processes that measure the amount of energy that cannot be used toward photosynthesis and heat dissipation causing potential damage to the leaf (PhiNO – fluorescence), the linear electron flow that is a proxy of photosynthesis (LEF), a calculated non-photochemical quenching (NPQt), and a leaf temperature differential that is the difference between the ambient temperature and the leaf temperature at the moment of measurement (LTD). All these parameters were also measured from 10:00 to 12:00 in the leaf

used for gas exchange and water potential measurements and in the other two leaves to have three replicates per individual.

During the weeks of Aug 16-26, I performed pressure-volume (PV) curves for individuals in the two opposite treatments of the experimental design (L- and H+) to measure four hydraulic traits that characterize the drought stress tolerance of a species. The PV curve gives the relationship between the leaf water potential (ψ_{leaf}, MPa) and the leaf relative water content (RWC). From its linear portion, we can determine the turgor loss point (ψ_{TLP}, MPa), the osmotic potential at full turgor (ψ_{100}, MPa), and the relative water content at the turgor loss point (RWC_{TLP}). From its non-linear portion, we can determine the modulus of elasticity of the cell walls (ε, MPa). We collected at 7 pm one leaf/needle per tree for *A. saccharum*, *B. alleghaniensis*, *Q. rubra*, and *P. resinosa* and a twig for *P. glauca*. The leaf/needle/twig was re-cut under water and covered with a black plastic bag to rehydrate overnight. The following day the leaf turgid fresh weight (LTFW, g) was measured with a 10^{-5} precision analytical scale (XSR205, Metler Toledo), and right after, the ψ_{leaf} was measured using a Scholander Pressure Chamber (Model 1505D-EXP/PMS- Instrument- Albany, OR). The leaves/needles were bench-dehydrated at ambient temperature. The fresh weight (LFW, g) and ψ_{leaf} were repetitively measured during the first 5 minutes every minute, then every 2 minutes for 10 minutes, and after that, every 5 minutes until the ψ_{leaf} stabilized. When the difference in water potential started increasing and the time between measurements was longer (5 min), we scanned the leaves to get their area (LA, cm^2). After the PV curve measurements were done, the leaves/needles were dried for 72 h at 65°C to get their dry weight (LDW, g). PV curves were analyzed using the PV curve fitting excel spreadsheet developed by Kevin P. Tu, Ph.D. It allows an automated assessment of the four hydraulic traits from the curves (https://landflux.org/tools).

The carbon 13 to carbon 12 isotope ratio ($\delta^{13}C$ ‰) is directly proportional to the water-use efficiency of the plant over the leaf's lifetime. This is because RUBISCO discriminates against carbon 13 isotopes, and it only binds it when stomata are closed, and carbon 12 has been depleted in the intercellular space (Lambers et al., 2008). The leaves used for the water potential measurements were also used to measure $\delta^{13}C$ through combustion conversion of 0.9-1.0mg of ground sample material to gas through a 4010 Elemental Analyzer (Costech Instruments, Italy) coupled to a Delta Plus XL (Thermo-Finnigan, Germany).

All plants were harvested between September 16 and 21, when leaves, stems, and roots were separated. All the leaves were collected and oven-dried during this harvest period for 72 h at 65 °C. Shed leaves before the harvest date were collected and dried to get the total mass invested toward leaf production. The dry mass of all the leaves was added, and the leaf mass fraction (LMF) was measured as the ratio of leaf dry mass to total plant dry mass.

Stem traits

At the stem level, I studied two morphological and physiological traits related to water transport, resource allocation, mechanical support, and storage (Table 1).

The Huber value (HV) is an integrative trait that relates the sapwood area to the leaf area providing information about the balance between water supply and loss and carbon allocation to leaves or stems. It has traditionally been measured with the sapwood area (fraction of xylem that conducts sap) as the numerator, although other dominators are now common. HV was measured on the distal branch of each tree as the ratio of sapwood area to leaf area. The sapwood area (m^2) was determined by measuring with a digital caliper the diameter at the base of the stem and the equation for the area of a circle. For all the species, I dried all the leaves/needless attached to the branch for 72 h at 65 °C to get their dry mass, and the total area was calculated from LMA.

The stem-specific density (SSD, mg mm^{-3}) has been shown to be at the intersection of four physiological functions: water safety, water efficiency, plant support, and resource storage (Chave et al., 2009). I took the average SSD of two wood segments along the main stem since SSD changes with wood age: a younger segment near the tip and an older segment near the base. The younger segment was cut right below the tip with a length of 5 cm. The older segment was determined by measuring a fixed distance from the tip and then cut to a length of 5 cm. The fixed distance was determined based on the shortest individual per species (*A. saccharum* = 16 cm, *B. alleghaniensis* = 54 cm, *P. glauca* = 11 cm, *P. resinosa* = 14 cm, and *Q. rubra* = 6 cm). The SSD of both segments was calculated as the stem section's dry masses divided by their volumes. The dry mass was obtained after drying each section for 72 h at 70°C. The volume was obtained using the water displacement method (Pérez-Harguindeguy et al., 2016). SSD of each tree was calculated as the average of the two segments.

Root traits

At the roots level, I studied five morphological and physiological traits involved in resource acquisition and conservation (Table 1).

After harvesting the trees, the whole root system of every individual was stored in sealed plastic bags along with some soil for five months in a -4°C freezer before processing. After five months, they were taken to a fridge for thawing without damaging the structure. The roots were manually washed in water until all soil was cleared. I selected at least ten fine-root replicates, defined here as 1^{st} to 3^{rd} order roots for all species. On these fine roots, I measured the following functional traits: specific root length (SRL, cm mg^{-1}), root mean diameter (RD, cm), root dry matter content (RDMC), root nitrogen content (RNC), and root carbon content (RCC). I scanned the fine roots using a flatbed scanner (STD4800; Regent Instruments Inc., Canada) at 1200 dpi. From these images, I calculated the fine root length, average fine root diameter, and fine root area per individual using WinRhizo (Reg. 2016a; Regent Instruments, Canada). Fine root fresh weights

were measured immediately after scanning, and dry weights were measured after 72 h of drying at 65°C. I determined C and N through combustion conversion of 1.1-1.2mg of ground sample material to gas through a 4010 Elemental Analyzer (Costech Instruments, Italy) coupled with a Delta Plus XL (Thermo-Finnigan, Germany). The remaining root system was dried for 72 h at 65°C to determine the total root mass. The root mass fraction (RMF) was calculated as the root total dry mass ratio to plant total dry mass.

Plant Performance

I measured plant performance using the relative growth rate (RGR) based on total biomass. To calculate the initial total plant biomass of the plants without killing them, I used a measure that combines total plant weight and soil weight at field capacity. At the start of the experiment (Initial Weight), I soaked the pots in water for 30 minutes after planting the trees in their pots, let them drain for 15 minutes, and then weighed them. I repeated this process at the end of the experiment (Final Weight). RGR was calculated as:

$$RGR = \frac{Ln(Final\ Weight) - Ln(Initial\ Weight)}{Ln(Initial\ Weight)} \qquad \textit{Eq. 2}$$

This method rests on the assumption that soil maintains its water-holding capacity throughout the experiment. Three individuals with negative growth values were removed from all analyses using RGR.

Statistical Analysis

All the statistical analyses were performed in R v4.1.3. The models' assumptions were verified using validation plots (Zuur et al., 2010; Zuur & Ieno, 2016). For all the statistical analyses showing a significant effect, the mean of each treatment are reported.

Objective 1: To evaluate the individual and combined effects of water deficit and heat on plant performance (RGR), I used a model of the form lm(RGR ~ Water + Temp + Water:Temp) per species (package{stats}, function(lm)). The interaction term between water deficit and heat (Water:Temp) was reported and included when statistically significant, and the individual effects of each stressor were not evaluated.

Objective 2: To evaluate which functional traits respond to water deficit and heat individually and both stresses combined, for each species, I used models of the form lm(Trait ~ Water +Temp + Water:Temp) (package{stats}, function(lm)), where "trait" represents each of the functional traits studied at the level of the leaf, stem, and roots. For those traits measured on different days, linear mixed models were used using heat (Temp) and drought (Water) as fixed effects and date (1|Date) as a random effect, following the form lmer(Trait ~ Water + Temp + Water:Temp + (1|Date) (package{lmerTest, nlme}, function(lmer)). The interaction term between water deficit and heat (Water:Temp) was reported and included when statistically significant and the

individual effects of each stressor were not evaluated. To evaluate the multivariate response, for each species I performed a Principal Component Analysis (PCA) on those traits that responded to water deficit and heat individually and combined. Additionally, I ran a redundancy analysis to assess how much of the variation in functional trait values can be explained by the water deficit and heat treatments individually and combined (package{vegan}, function(rda)).

Objective 3: I performed a four steps analysis to evaluate which functional traits mediate the performance response to water deficit and heat. Each of the steps was individually performed for each species, and only those traits that significantly responded to water deficit and heat were included in these analyses (Objective 2). First, I calculated the change in functional trait and relative growth rate values under MWD and HWD relative to LWD, because I was interested in the effect of change in functional trait values on the maintenance of plant performance. I did not distinguish based on temperature treatment because only the water deficit treatment affected species' relative growth rate. The change in functional trait values was calculated as follows:

$$\Delta FT = \left| \frac{\overline{FT_{LWD}} - FTi_{MWD\ \&\ HWD}}{\overline{FT_{LWD}}} \right| \qquad \textit{Eq. 3}$$

$\overline{FT_{LWD}}$ represents the mean trait value under LWD and $FTi_{MWD\ \&\ HWD}$ represents the observed trait value for every individual in the MWD and HWD treatments, with a samples size s of n=24 per species. The change in relative growth rate was calculated as follows:

$$\Delta RGR = \frac{\overline{RGR_{LWD}} - RGRi_{MWD\ \&\ HWD}}{\overline{RGR_{LWD}}} \qquad \textit{Eq. 4}$$

Using $\overline{RGR_{LWD}}$, the mean relative growth rate under LWD and $RGRi_{MWD\ \&\ HWD}$, the observed relative growth rate for every individual in the MWD and HWD treatments, we obtained a sample size for ΔRGR of n=24 per species.

Second, I tested which trait changes were associated with changes in plant performance. To do so, I used Spearman's correlation coefficient to determine if functional traits and relative growth rate were correlated.

Third, to assess the individual effect of traits that responded to water deficit and heat, I performed a mixed linear regression for each trait that showed a significant response in objective 2 following the form lmer(ΔRGR ~ ΔFT + (1|Water) (package{lmerTest, nlme}, function(lmer)).

Fourth, to assess the joint effect of multiple traits, I built a multiple regression mixed linear model following the form lmer(ΔRGR ~ ΔFT_1 … ΔFT_n + (1|Water)) (package{lmerTest, nlme}, function(lmer)). Because there were only 24 observations and more than five functional traits that responded for each species, I performed a model selection process by AIC using a stepwise

algorithm in both directions (package{stats}, function(step)). The random effect (1|Water) was dropped when non-significant, and I performed a linear model with the change in functional traits and performance instead. I only interpreted the negative correlations between ΔRGR and ΔFT because big changes in functional traits should be associated with mitigating performance reduction under stressful environmental conditions. This approach is valid in the current context because RGR is bound between 0 and 1, such that a negative correlation means a large change in trait value associated with a small change in RGR.

Results

Effectiveness of the treatments on environmental conditions

The three deficit water levels resulted in significantly different volumetric water contents among the three treatments ($F_{(2,77.9)}$ = 58.2, p = 2.2e-15, μ_{LWD} = 38.2%, μ_{MWD} = 35.7%, μ_{HWD} = 31.3%, Figure 3). The OTCs resulted in a significant average increase of 0.42 °C throughout the day, with the most pronounced warming during the evening (17h00 – 20h00, + 0.48°C), night (20h00 – 6h00, + 0.64°C), and morning (6h00 – 13h00, 0.6°C), and no warming effects from 13h00 to

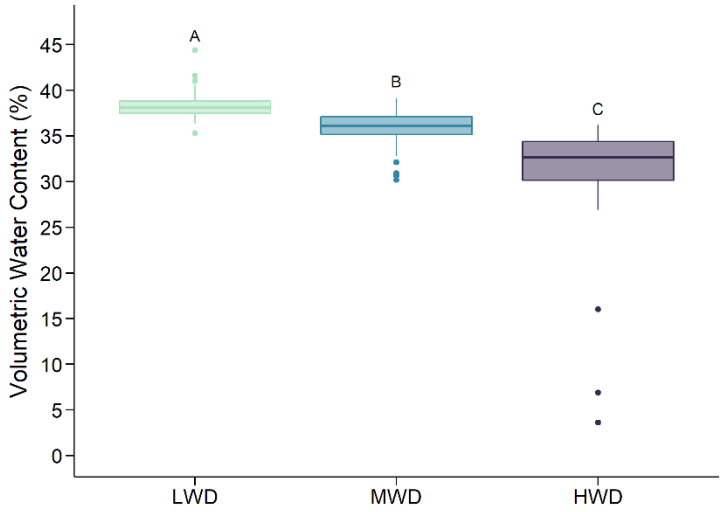

17h00 ($F_{(1,83.0)}$ = 17.8, p = 6.1e-5, $\mu_{w/oOTC}$ = 24.4 °C, μ_{OTC} = 24.8 °C, Figure 4).

Figure 3. Differences in water deficit treatments. Volumetric water content (%) under low water deficit (LWD), medium water deficit (MWD), and high-water deficit (HWD). Letters denote statistically significant differences between treatments.

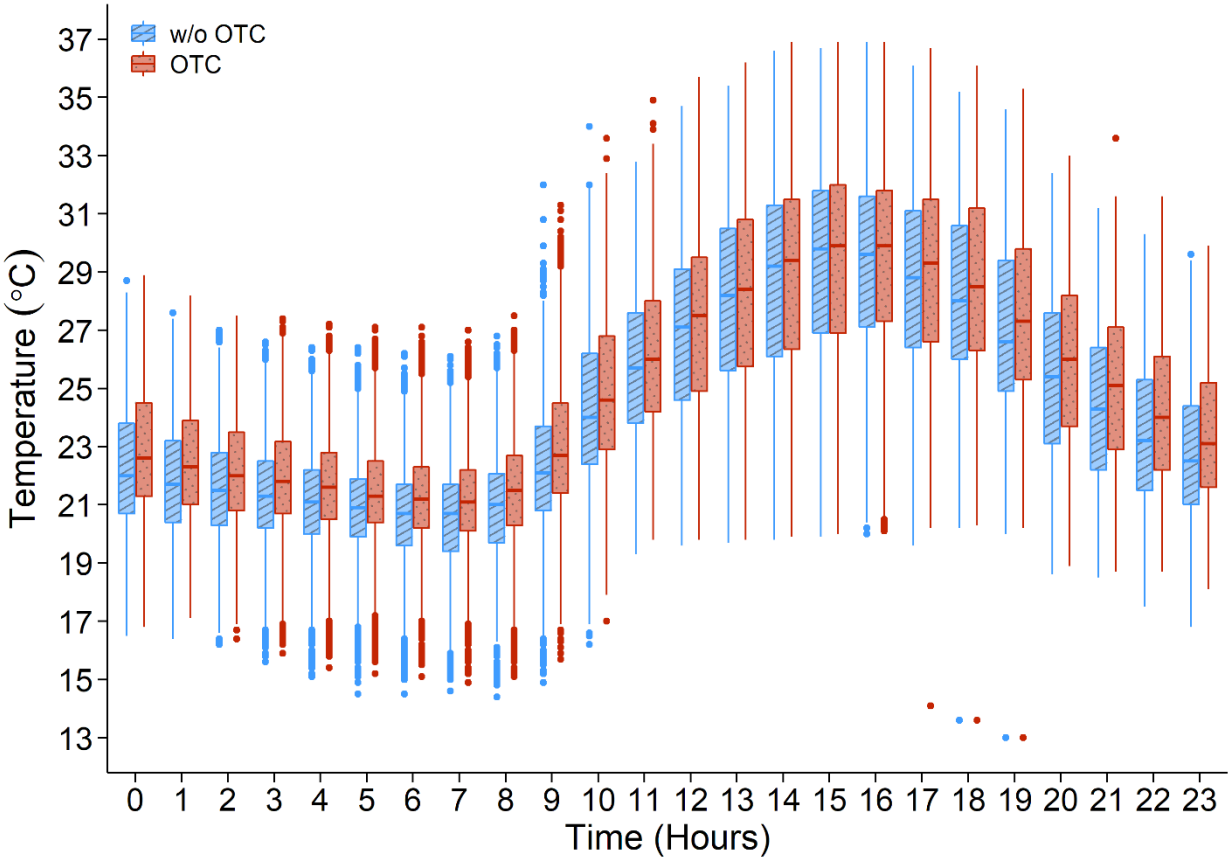

Figure 4. Difference in temperature between treatments with and without open-top chambers (OTC). Averaged temperature values along the day throughout the entire experiment showing the temperature of plants exposed to ambient temperature (without OTC, blue boxes) vs. plants exposed to warmer temperatures using OTCs (with OTC, red boxes).

Objective 1 – What are water deficit and heat's individual and combined effects on plant performance (RGR)?

All species showed a reduction in RGR with water deficit. For the broadleaves species, RGR in the MWD and HWD treatments were equal to each other and 36 to 55% lower than in the LWD treatment (*A. saccharum*: $F_{(2,32)}$ = 19.83, p = 2.49e-6, μ_{LWD} = 1.44e-2, μ_{MWD} = 7.83e-3, μ_{HWD} = 6.47e-3; *B. alleghaniensis:* $F_{(2,30)}$ = 13.81, p = 5.59e-5, μ_{LWD} = 1.75e-2, μ_{MWD} = 1.04e-2, μ_{HWD} = 9.64e-3; *Q. rubra:* $F_{(2,31)}$ = 35.48, p = 9.66e-9, μ_{LWD} = 1.57e-2, μ_{MWD} = 1.0e-2, μ_{HWD} = 8.33e-3, Figure 5). In the broadleaf species, the temperature did not affect RGR. RGR decreased by 26 to 45% with water deficit for both conifer species, with values under the HWD treatment being significantly lower than that under the LWD treatment (*P. glauca*: $F_{(2,31)}$ = 5.86, p = 6.95e-3, μ_{LWD} = 1.83e-2, μ_{MWD} = 1.32e-2, μ_{HWD} = 1.05e-2*; P. resinosa:* $F_{(2,30)}$ = 7.23, p = 2.68e-3, μ_{LWD} = 1.5e-2, μ_{MWD} = 1.1e-2, μ_{HWD} = 8.2e-3, Figure 5). Additionally, increased temperature increased the RGR of *P. glauca* but did not affect *P. resinosa* (*P. glauca*: $F_{(1,31)}$ = 4.09, p = 5.2e-2, $\mu_{w/oOTC}$ = 1.21e-2, μ_{OTC} =1.59e-2, Figure 5). In none of the species did water deficit and temperature interact to affect RGR.

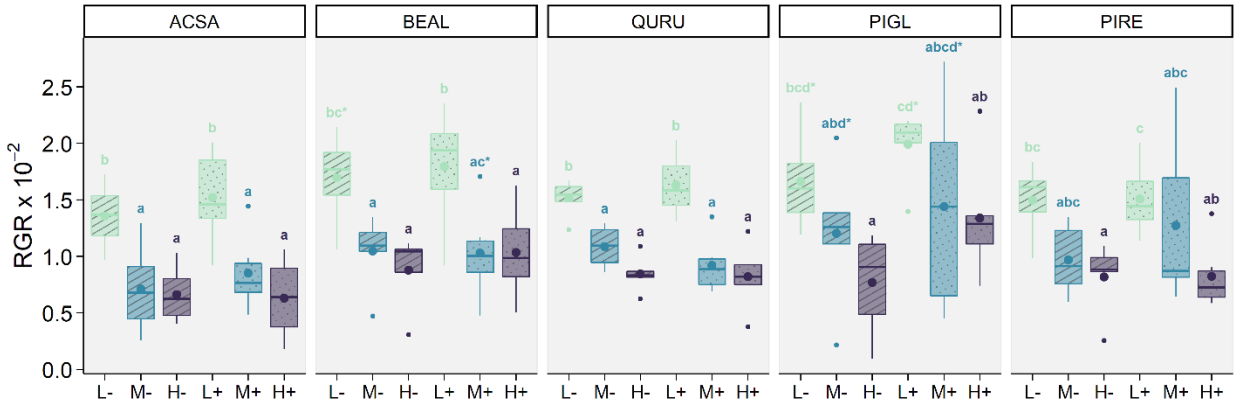

Figure 5. RGR of *A. saccharum* (ACSA), *B. alleghaniensis* (BEAL), *Q. rubra* (QURU), *P. glauca* (PIGL), and *P. resinosa* (PIRE) under six different treatments of water deficit and heat. Letters denote statistically significant differences between treatments. Similar letters followed by an * indicate that the treatments are equal for an alpha=0.05 while different for an alpha=0.1. Line in the box plots indicates the median values, whereas solid dots indicate the mean values.

Objective 2 – Which functional traits respond to water deficit, heat stress, and both?
In general, the drought treatment affected fewer traits than the heat treatment. Further, each species showed different phenotypic responses to those two stresses (Table S1).

The only shared trait response to heat across species is in their leaf cooling (LTD, Figure 6). Individuals in the warmer treatment showed a lower leaf temperature relative to ambient (*A. saccharum:* $F_{(1,32)}$ = 8.77, p = 5.7e-3, $\mu_{w/oOTC}$ = -1.84, μ_{OTC} = -3.55*; B. alleghaniensis:* $F_{(1,31.1)}$ = 8.18, p = 7.5e-3, $\mu_{w/oOTC}$ = -3.18, μ_{OTC} = -4.45*; Q. rubra:* $F_{(1,29.6)}$ = 4.21, p = 4.9e-2, $\mu_{w/oOTC}$ = -2.68, μ_{OTC} = -3.82*; P. glauca:* $F_{(1,28.6)}$ = 5.41, p = 2.7e-2, $\mu_{w/oOTC}$ = -1.50, μ_{OTC} = -2.21*; P. resinosa:* $F_{(1,26.9)}$ = 9.67, p = 4.3e-3, $\mu_{w/oOTC}$ = -2.92, μ_{OTC} = -4.69). Since all other phenotypic changes were unique to each species, below I discuss the remainder of these changes' species by species.

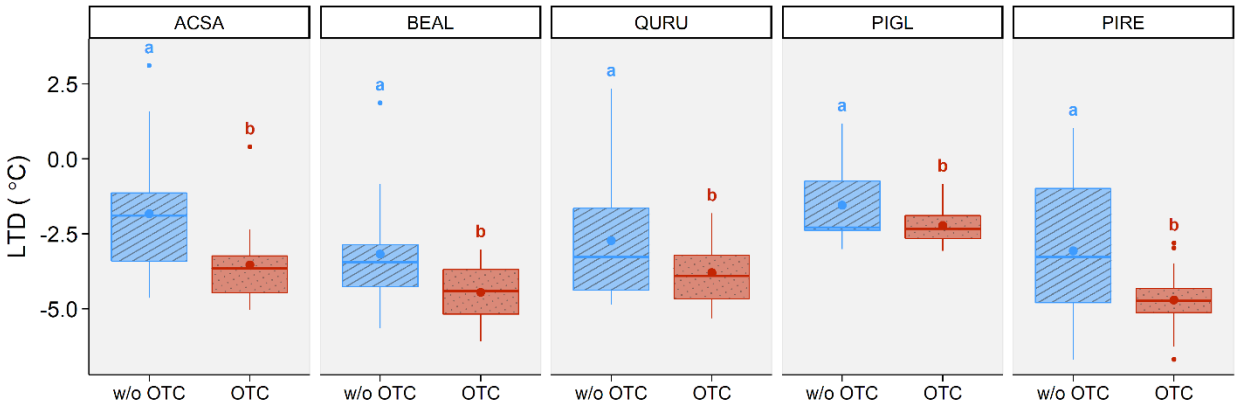

Figure 6. Difference between leaf temperature differential in ambient temperature (w/o OTC) and warmer temperature conditions (OTC) for *A. saccharum* (ACSA), *B. alleghaniensis* (BEAL), *Q. rubra* (QURU), *P. glauca* (PIGL), and *P. resinosa* (PIRE). Letters denote

statistically significant differences between treatments. Similar letters followed by an * indicate that the treatments are equal for an alpha=0.05 while different for an alpha=0.1. Line in the box plots indicates the median values, whereas solid dots indicate the mean values.

A. saccharum

In *A. saccharum,* four functional traits from all organs responded to individual water deficit and heat stresses. The response to water deficit was conditional on heat in four leaf traits (Tables 2 and S1).

Table 2. *A. saccharum* summary table of functional traits that responded to the stresses imposed. The parenthesis information indicates the direction of change as a percentage relative to LWD for water deficit, relative to w/o OTC for temperature, and relative to both stresses for the combined treatment.

Stress	Trait
Water deficit	RDMC (+22.9% MWD)
	SSD (-6.3% MWD & -11% HWD)
Heat	LTD (+92.9% OTC)
Water deficit + Heat	RWC_{TLP} (-7.3% H+)
Interaction	LT
	LMA
	g_s
	E

Response to Water Deficit

In *A. saccharum*, stem specific density and root dry matter content changed in response to water deficit, with the largest response shown by RDMC. Stem specific density decreased by 6.3% and 11% under MWD and HWD relative to LWD, respectively (SSD, $F_{(2,32)} = 15.94$, $p = 1.58e\text{-}5$, $\mu_{LWD} = 0.718$, $\mu_{MWD} = 0.673$, $\mu_{HWD} = 0.639$; Figure 7A). Root dry matter content increased 22.9% under MWD compared to LWD (RDMC: $F_{(2,32)} = 4.80$, $p = 1.5e\text{-}2$, $\mu_{LWD} = 0.15$, $\mu_{MWD} = 0.19$, $\mu_{HWD} = 0.17$; Figure 7B), but did not show a significant change under HWD.

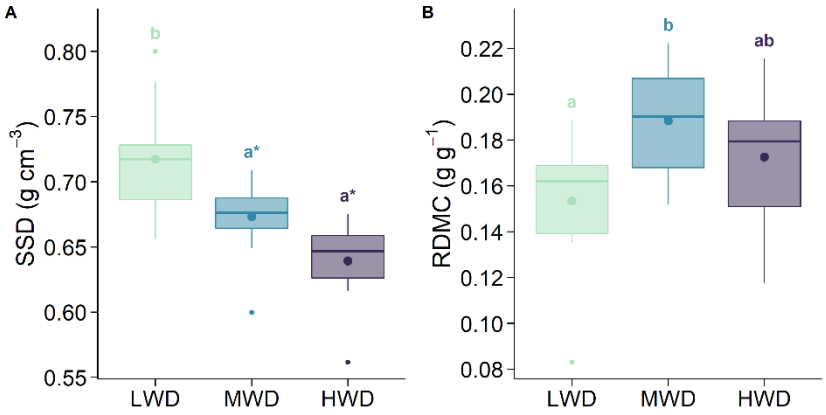

Figure 7. *A. saccharum*'s functional traits that responded to water deficit: stem specific density (SSD, A) and root dry matter content (RDMC, B). Letters denote statistically significant differences between treatments. Similar letters followed by an * indicate that the treatments are equal for an alpha=0.05 while different for an alpha=0.1. Line in the box plots indicates the median values, whereas solid dots indicate the mean values.

Response to both Water Deficit and Heat

The relative water content at turgor loss point decreased by 7.3 % in H+ relative to L- (RWC_{TLP}: $F_{(1,9)}$ = 5.60, p = 4.2e-2, μ_{L-} = 0.903, μ_{H+} = 0.837; Figure 8). The water potentials at turgor loss point (ψ_{TLP}) and at full turgor (ψ_{100}) showed a non-significant tendency towards lower values under H+ (ψ_{TLP}: $F_{(1,9)}$ = 1.9, p= 0.20, μ_{L-} = -1.13, μ_{H+} = -1.43; ψ_{100}: $F_{(1,9)}$ = 1.80, p= 0.21, μ_{L-} = -0.82, μ_{H+} = -1.1, Figure 8).

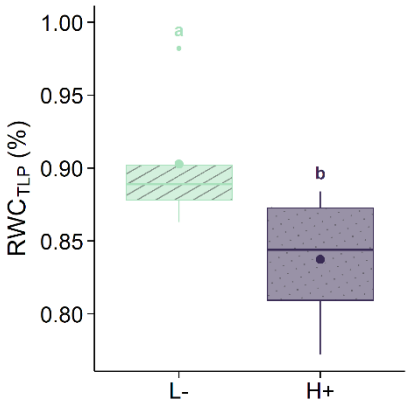

Figure 8. *A. saccharum*'s functional traits that responded to both water deficit and heat: relative water content at turgor loss point (RWC_{TLP}). Letters denote statistically significant differences between treatments. Line in the box plots indicates the median values, whereas solid dots indicate the mean values.

Response to Water Deficit conditional on Heat

Four morphological and physiological traits of *A. saccharum* associated with resource use showed interaction in their response to water deficit and heat. Three traits showed opposite responses to water deficit in the control and warmed treatments.

Leaves where thinner in all treatments compared to L- conditions (LT: $F_{(2,30)}$ = 2.48, p= 0.10, μ_{L-} = 1.51e-1, μ_{M-} = 1.29e-1, μ_{H-} = 1.29e-1, μ_{L+} = 1.32e-1, μ_{M+} = 1.28e-1, μ_{H+} = 1.31e-1, Figure 9A). In ambient temperature conditions (-), leaf mass per area increased under MWD and HWD compared to LWD, while in warmer temperature conditions (+) it decreased from LWD to HWD (LMA: $F_{(2,30)}$ = 3.80, p = 3.4e-2, μ_{L-} = 33.3, μ_{M-} = 36.7, μ_{H-} = 36.3, μ_{L-} = 39.1, μ_{M-} = 37.9, μ_{H+} = 34.4, Figure 9B). Individuals under L+ conditions had smaller leaves with higher mass per area than individuals under L- conditions.

In ambient temperature conditions (-) both stomatal conductance and transpiration rate showed a marginal increase under HWD compared to LWD and MWD, while in warmer temperature conditions they marginally decrease under HWD compared to LWD and MWD (g_s: $F_{(2,26.1)}$ = 2.77, p = 8.0e-2, μ_{L-} = 3.93e-2, μ_{M-} = 4.46e-2, μ_{H-} = 6.16e-2, μ_{L-} = 5.22e-2, μ_{M-} = 5.59e-2, μ_{H+} = 3.06e-2; E: $F_{(2,26.1)}$ = 2.67, p = 8.7e-2, μ_{L-} = 0.62, μ_{M-} = 0.69, μ_{H-} = 0.94, μ_{L-} = 0.80, μ_{M-} = 0.84, μ_{H+} = 0.47, Figure 9C-D).

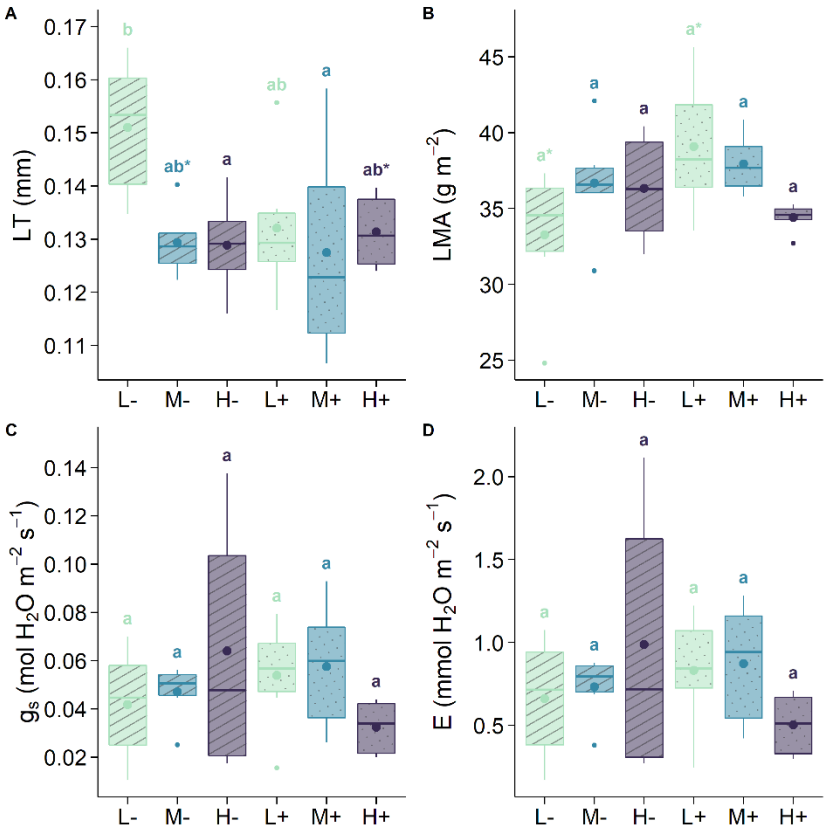

Figure 9. *A. saccharum*'s functional traits that showed a response to water deficit conditional on heat: leaf thickness (LT, A), leaf mass per area (LMA, B), stomatal conductance (g_s, C), and

transpiration rate (E, D). Letters denote statistically significant differences between treatments. Similar letters followed by an * indicate that the treatments are equal for an alpha=0.05 while different for an alpha=0.1. Line in the box plots indicates the median values, whereas solid dots indicate the mean values.

Multivariate response to water deficit and heat

The three first axes of variation were significant and explained 77.5% of the variation in functional traits among individuals and treatments (Figure 10). In *A. saccharum*, principal component 1 is significantly correlated with stomatal conductance (r = 0.96, p = 8.41e-21), transpiration rate (r = 0.96, p = 5.57e-20), and the leaf mass per area (r = 0.58, p = 2.29e-4). All those are leaf traits associated with plant resource acquisition, water transport, and thermoregulation. Principal component 2 is significantly correlated with stem specific density (r = 0.76, p = 8.22e-8), leaf thickness (r = 0.60, p = 9.99e-5), root dry matter content (r = -0.79, p = 6.84e-9). These three traits belong to three different organs and are associated with resource acquisition and conservation, water transport, mechanical support, and storage. Based on the redundancy analysis, water deficit and heat individually and combined explained 15% of the variation in functional traits values ($F_{(5,30)}$ = 2.24, p = 0.004), with the effect of water deficit (p = 0.05) being significant, and the effect of heat (p = 0.076) and water deficit conditional on heat (p = 0.071) being marginally significant.

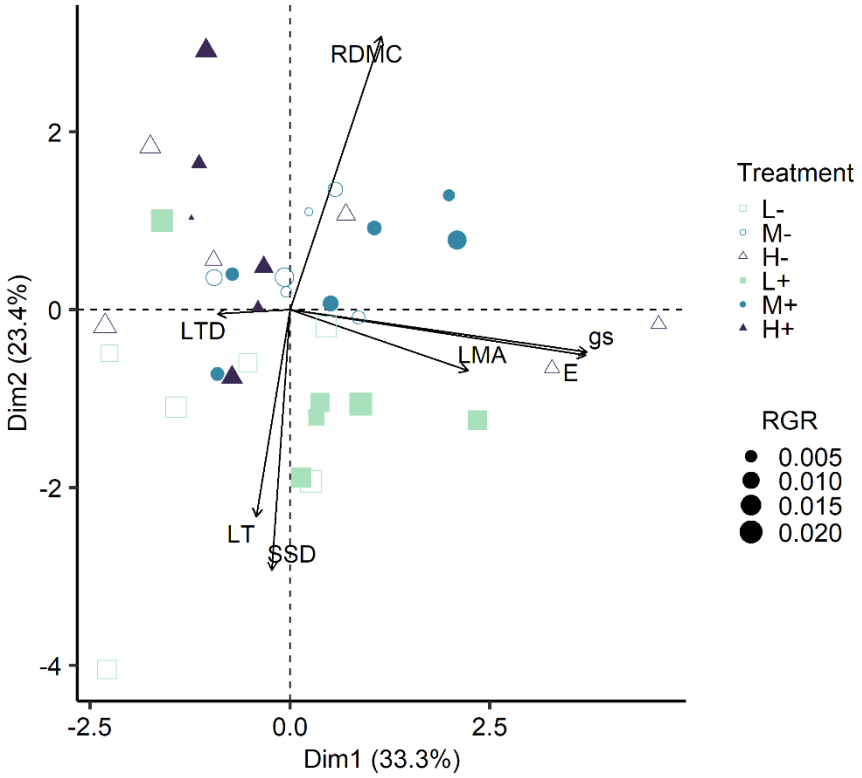

Figure 10. *A. saccharum*'s PCA including all the functional traits that responded to water deficit, heat, and water deficit conditional on heat. Open symbols corresponded to individuals under ambient temperature conditions (without OTC, -), while solid symbols correspond to individuals under warmer conditions (with OTC, +). The green squares correspond to LWD, the blue circles to MWD, and the purple triangles to HWD conditions. The size of the symbols indicates their RGR

B. alleghaniensis

B. alleghaniensis was the species that responded the least to water deficit and heat, with only six traits from all organs showing a response. Only leaf traits responded to water deficit and heat stresses alone. Stem and root traits responded differently to water deficit depending on heat (Tables 3 and S1).

Table 3. *B. alleghaniensis* summary table of functional traits that responded to the stresses imposed. The parenthesis information indicates the direction of change as a percentage relative to LWD for water deficit, relative to w/o OTC for temperature, and relative to both stresses for the combined treatment.

Stress	Trait
Water deficit	LTD (+40.1 HWD)
Heat	LTD (+39.9% OTC)

	NPQt (-18.5% OTC)
	PhiNPQ (-12.4% OTC)
	PhiNO (+5.1% OTC)
Interaction	SSD
	RMF

Response to Water Deficit

The leaf cooling response showed non-linear responses, with individuals under MWD having leaf temperatures closer to air temperature. This led to a marginal increase by 40.1% in the leaf temperature differential under HWD relative to MWD ($F_{(2,27.9)}$ = 3.02, p = 6.5e-2, μ_{LWD} = -4.15,

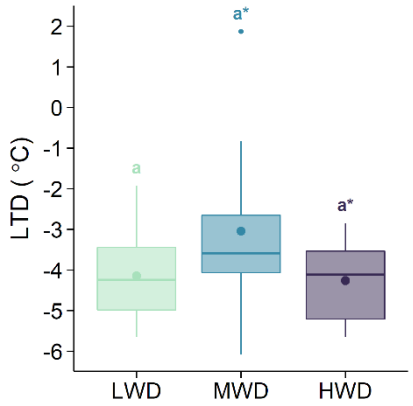

μ_{MWD} = -3.04, μ_{HWD} = -4.26*;* Figure 11).

Figure 11. *B. alleghaniensis*'s functional traits that responded to water: leaf temperature differential (LTD). Letters denote statistically significant differences between treatments. Similar letters followed by an * indicate that the treatments are equal for an alpha=0.05 while different for an alpha=0.1. Line in the box plots indicates the median values, whereas solid dots indicate the mean values.

Response to Heat

Traits associated with the photosynthetic apparatus status were affected by warmer temperatures showing a reduction of 18.5% in the calculated amount of light dissipated as heat (NPQt: $F_{(2,32)}$ = 4.95, p = 3.3e-2, $\mu_{w/oOTC}$ =0.82, μ_{OTC} = 0.67; Figure 12A), a reduction of 12.4% in the fraction of light energy allocated towards heat dissipation (PhiNPQ: $F_{(2,32)}$ = 4.26, p = 4.7e-2, $\mu_{w/oOTC}$ =0.17, μ_{OTC} =0.15, Figure 12B), and an increase of 5.1% in the amount of energy allocated towards fluorescence (PhiNO: $F_{(2,29.0)}$ = 4.67, p = 3.9e-2, $\mu_{w/oOTC}$ = 0.22, μ_{OTC} =0.23; Figure 12C).

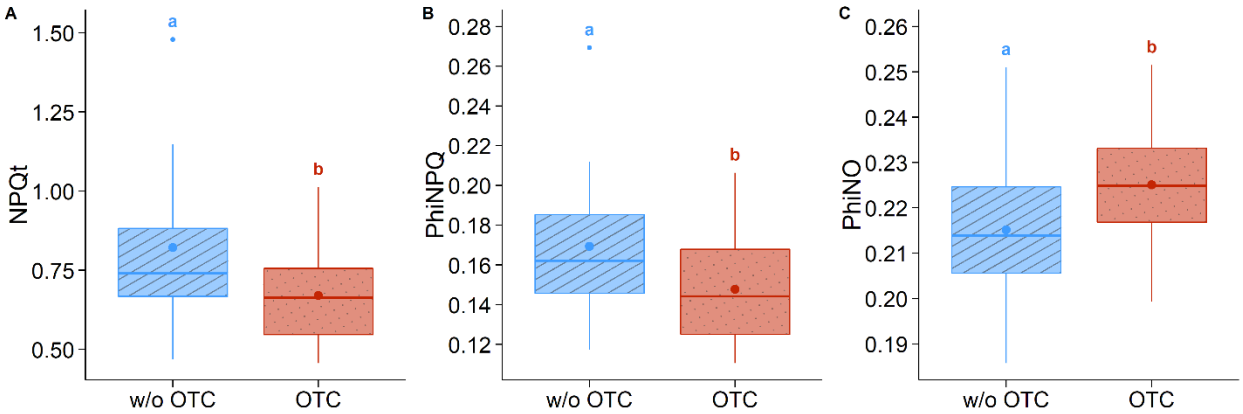

Figure 12. *B. alleghaniensis*'s functional traits that respond to heat: non-photochemical quenching (NPQt, A), the ratio of incoming light that goes towards non-photochemical quenching (PhiNPQ, B), and the ratio of incoming light that is lost via non-regulated processes (PhiNO, C). Letters denote statistically significant differences between treatments. Line in the box plots indicates the median values, whereas solid dots indicate the mean values.

Response to Water Deficit conditional on Heat

B. alleghaniensis showed interaction in the response of stem-specific density and root mass fraction to water deficit and heat.

SSD showed opposite non-linear responses to water deficit in the ambient and warmed conditions: under ambient temperature conditions, the MWD treatment showed the lowest stem density, while under warmer temperatures, the MWD treatment showed the highest stem density. The trees under M- conditions had lower stem density than trees under L- (p = 0.05), H-, M+, and H+ (p = 0.07), and tress under M+ conditions had higher stem density than trees under L+ conditions (SSD: $F_{(2,30)}$ = 13.21, p = 7.67e-5, μ_{L-} = 0.72, μ_{M-} = 0.64, μ_{H-} = 0.72, μ_{L+} = 0.66, μ_{M+} = 0.76, μ_{H+} = 0.71; Figure 13A).

RMF showed a linear but opposite response to water deficit under ambient and warmed conditions: the HWD treatment showed the highest root mass fraction under ambient temperature conditions. In contrast, the HWD treatment showed the lowest root mass fraction under warmer temperatures. The trees under H- conditions had higher root mass fractions than trees under H+ (RMF: $F_{(2,32)}$ = 3.33, p = 4.94e-2, μ_{L-} = 0.31, μ_{M-} = 0.33, μ_{H-} = 0.34, μ_{L+} = 0.32, μ_{M+} = 0.31, μ_{H+} = 0.29; Figure 13B).

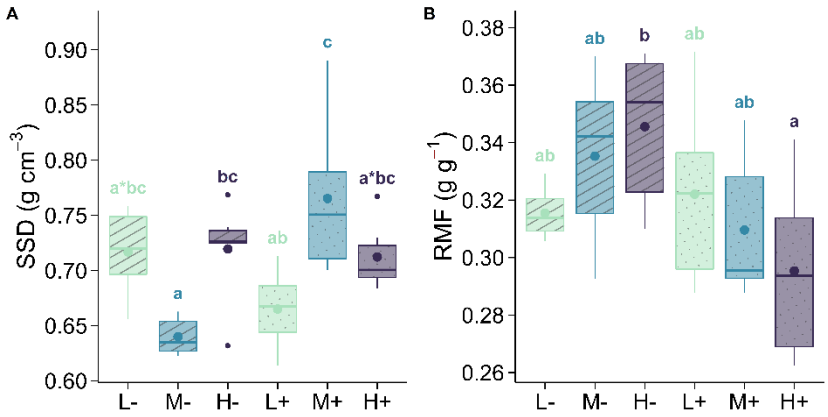

Figure 13. *B. alleghaniensis*'s functional traits that showed a response to water deficit conditional on heat: stem specific density (SSD, A), root mass fraction (RMF, B). Letters denote statistically significant differences between treatments. Similar letters followed by an * indicate that the treatments are equal for an alpha=0.05 while different for an alpha=0.1. Line in the box plots indicates the median values, whereas solid dots indicate the mean values.

Multivariate response to water deficit and heat

The first axis of variation was significant and explained 48.5% of the variation in functional traits among individuals and treatments (Figure 14). In *B. alleghaniensis*, principal component 1 is significantly correlated with the calculated non-photochemical quenching (r = 0.97, p = 5.14e-23), the amount of light towards non photochemical quenching (r = 0.95, p = 1.12e-18), the leaf temperature differential (r = 0.55, p = 5.44e-4), and the amount of light energy allocated towards non-regulated processes (r = -0.83, p = 4.33e-10). All those are leaf traits associated with photo and thermoregulation. Principal component 2 is significantly correlated with root mass fraction (r = 0.7, p = 2.08e-6), leaf temperature differential (r = 0.47, p = 3.71e-3), and stem specific density (r = -0.74, p = 1.87e-7). These three traits belong to three different organs and are associated with resource acquisition and conservation, thermoregulation, support, and storage. Based on the redundancy analysis, water deficit and heat individually and combined explained 16.9% of the variation in functional traits values ($F_{(5,30)}$ = 2.42, p = 0.004) with the effect of heat (p = 0.001) and water deficit conditional on heat (p = 0.016) being significant.

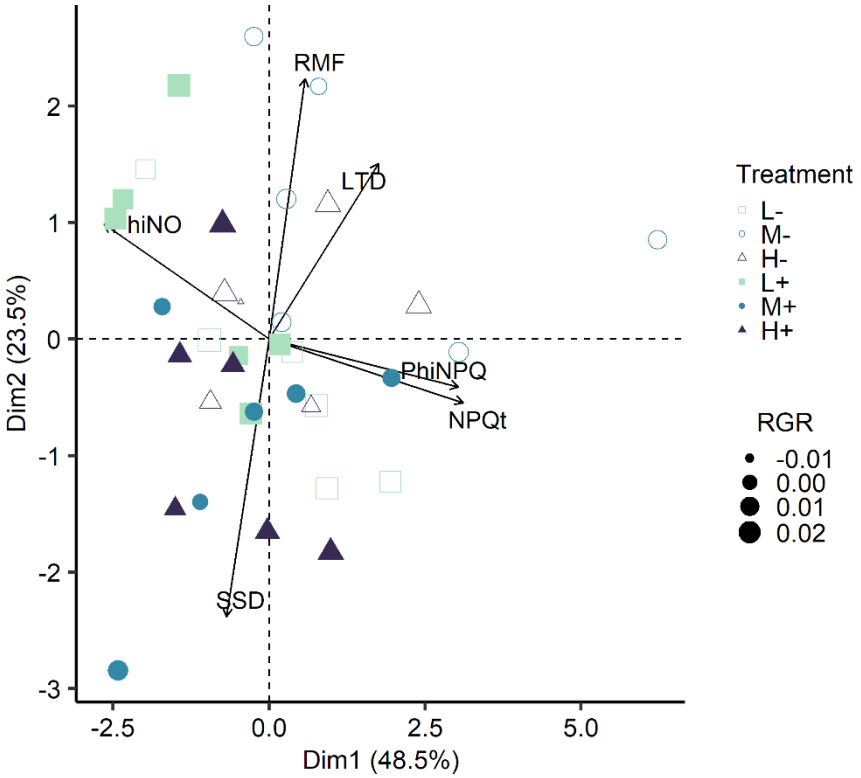

Figure 14. *B. alleghaniensis*'s PCA including all the functional traits that responded to water deficit, heat, and water deficit conditional on heat. Open symbols corresponded to individuals under ambient temperature conditions (without OTC), while solid symbols correspond to individuals under warmer conditions. The green squares correspond to LWD, the blue circles to MWD, and the purple triangles to HWD conditions. The size of the symbols indicates their RGR.

Q. rubra

In *Q. rubra*, 14 functional traits from all organs showed responses to water deficit and heat stress, with 6 of the 14 traits showing strong responses of effect sizes between 35 to 60%. Leaf, stem, root, and whole-plant traits responded to water deficit. Leaf and root traits responded to heat, the combination of water deficit and heat, and to water deficit conditional on heat (Tables 4 and S1).

Table 4. *Q. rubra* summary table of functional traits that showed a response to the stresses imposed. The parenthesis information indicates the direction of change as a percentage relative to LWD for water deficit, relative to w/o OTC for temperature, and relative to both stresses for the combined treatment.

Stress	Trait
Water deficit	ψ_{PD} (-45% HWD)

	HV (+39.1 – 49.1% HWD)
	$\Delta\psi$ (-37.4% MWD & -43.1% HWD)
	A_{MAX}^{M} (-29.1% HWD)
	A_{MAX}^{A} (-27.1% HWD)
	ψ_{MD} (+18.4% MWD)
	RMF (+11.9 – 12.8% HWD)
Heat	LTD (+42.5% OTC)
	WUE (-14.4 % OTC)
	WUEi (-14% OTC)
	RDMC (-13.3% OTC)
	RMF (-10.9% OTC)
Water deficit + Heat	ε (+68% H+)
	ψ_{100} (-34.6% H+)
Interaction	LT

Response to Water Deficit

Q. rubra's predawn water potential, midday water potential, the difference between water potentials, maximum carbon assimilation per area and mass, Huber value, and root mass fraction showed a response to water deficit.

Predawn water potential decreased by 45% from LWD to HWD (ψ_{PD}: $F_{(2,27.9)}$ = 3.72, p = 3.69e-2, μ_{LWD} = -0.22, μ_{MWD} = -0.27, μ_{HWD} = -0.32; Figure 15A). Midday water potential under the MWD showed a 18.4% marginal increase compared to the LWD water potentials (ψ_{MD}: $F_{(2,27.8)}$ = 2.64, p = 8.9e-2, μ_{LWD} = -0.72, μ_{MWD} = -0.59, μ_{HWD} = -0.60; Figure 15B). Shifts in predawn and midday water potentials led to decreases of 37.4 and 43.1% in their difference under MWD and HWD ($\Delta\psi$: $F_{(2,27.7)}$ = 6.71, p= 4.2e-3, μ_{LWD} = -0.50, μ_{MWD} = -0.31, μ_{HWD} = -0.29; Figure 15C).

Maximum carbon assimilation per area and mass showed non-linear responses, with values under MWD conditions being marginally higher than under HWD. These two traits decreased 27.1% and 29.1%, respectively, under HWD compared to MWD (A_{MAX}^{A}: $F_{(2,28.8)}$ = 2.43, p = 0.10, μ_{LWD} = 4.34, μ_{MWD} = 4.87, μ_{HWD} = 3.55; Figure 15D. A_{MAX}^{M}: $F_{(2,28.5)}$ = 3.00, p = 6.6e-2, μ_{LWD} = 100.0, μ_{MWD} = 112.6, μ_{HWD} = 79.8; Figure 15E).

The Huber value increased under HWD compared to LWD and MWD by 39.3% and 49.1%, respectively (HV: $F_{(2,27.9)}$ = 5.44, p = 9.22e-3, μ_{LWD} = 2.29e-4, μ_{MWD} = 2.14e-4, μ_{HWD} = 3.19e-4, Figure 15F).

Root mass fraction was marginally higher under HWD relative to both LWD and MWD by 12.8% and 11.9%, respectively (RMF_{WD}: $F_{(2,32)}$ = 3.32, p = 4.89e-2, μ_{LWD} = 0.52, μ_{MWD} = 0.53, μ_{HWD} = 0.59, Figure 15G).

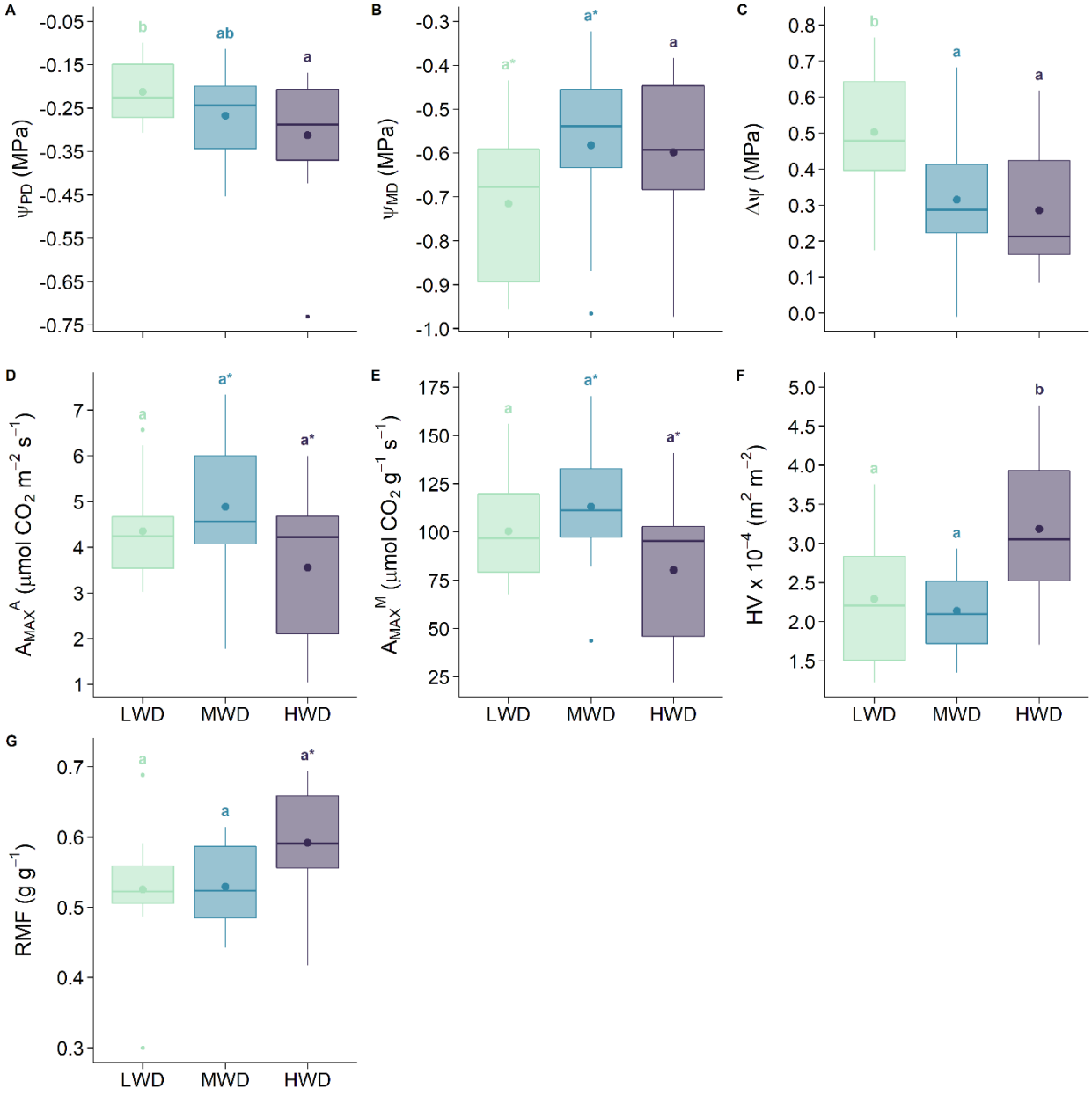

Figure 15. *Q. rubra*'s functional traits that responded to water deficit: predawn water potential (ψ_{PD}, A), midday water potential (ψ_{MD}, B), the difference between ψ_{PD} and ψ_{MD} ($\Delta\psi$, C), maximum carbon assimilation per area (A_{MAX}^{A}, D), maximum carbon assimilation per mass

(A_{MAX}^{M}, E), Huber value (HV, F), and root mass fraction (RMF, G). Letters denote statistically significant differences between treatments. Similar letters followed by an * indicate that the treatments are equal for an alpha=0.05 while different for an alpha=0.1. Line in the box plots indicates the median values, whereas solid dots indicate the mean values.

Response to Heat

Q. rubra's instantaneous water use efficiency, intrinsic water use efficiency, root dry matter content, and root mass fraction showed a response to heat.

Instantaneous and intrinsic water use efficiency showed a reduction of 14.4% and 14%, respectively, under warmer temperature conditions (WUE: $F_{(1,32)}$ = 10.69, DF = 1, p = 2.6e-3, $\mu_{w/oOTC}$ = 5.68, μ_{OTC} = 4.86; WUEi: $F_{(1,32)}$ = 9.64, p= 4.0e-3, $\mu_{w/oOTC}$ = 86.3, μ_{OTC} = 74.2; Figure 16A-B).

Root dry mater content and root mass fraction diminished by 13.8% and 10.9%, respectively, under warmer temperatures (RDMC: $F_{(1,32)}$ = 5.8, p = 2.2e-2, $\mu_{w/oOTC}$ = 0.3, μ_{OTC} = 0.26; RMF:

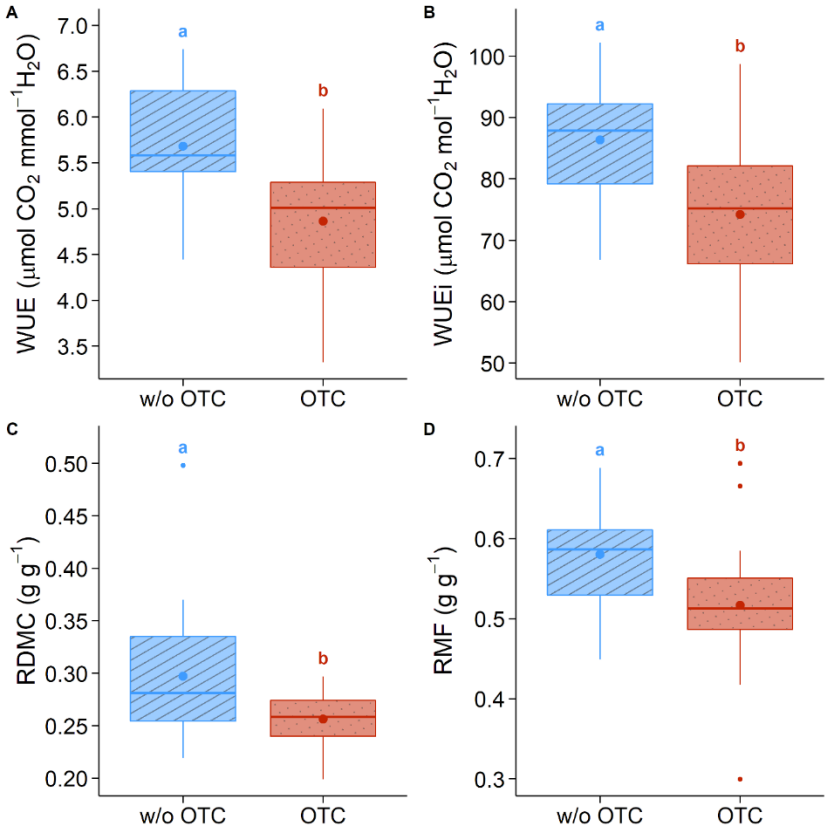

$F_{(1,32)}$ = 7.27, p= 1.1e-2, $\mu_{w/oOTC}$ = 0.58, μ_{OTC} = 0.52, Figure 16C-D).

Figure 16. *Q. rubra*'s functional traits that responded to heat: instantaneous water use efficiency (WUE, A), intrinsic water use efficiency (WUEi, B), root dry matter content (RDMC, C), and root mass fraction (RMF, D). Letters denote statistically significant differences between

treatments. Letters denote statistically significant differences between treatments. Line in the box plots indicates the median values, whereas solid dots indicate the mean values.

Response to both Water Deficit and Heat

Q. rubra showed an osmotic adjustment by reducing water potential at full turgor by 34.6% and increasing cell walls elasticity by 68% under H+ compared to L- (ψ_{100}: $F_{(1,7.1)}$ = 6.60, p = 3.7e-2, μ_{L-} = -0.7, μ_{H+} = -0.94; Figure 17A. ε: $F_{(1,8.4)}$ = 9.73, p = 0.013, μ_{L-} = 1.28, μ_{H+} = 2.15; Figure 17B).

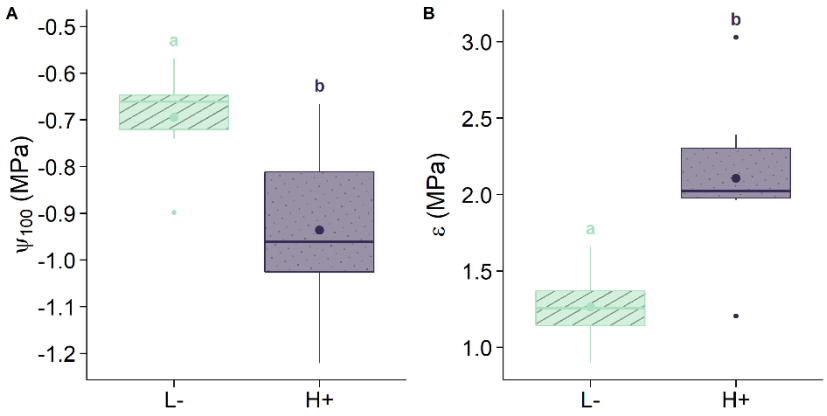

Figure 17. *Q. rubra*'s functional traits that responded to both water deficit and heat without considering all the treatments: osmotic potential at full turgor (ψ_{100}, A) and the modulus of elasticity (ε, B). Letters denote statistically significant differences between treatments. Line in the box plots indicates the median values, whereas solid dots indicate the mean values.

Response to Water Deficit conditional on Heat

Leaf thickness showed an interaction in is response to water deficit and heat (LT: $F_{(2,30)}$ = 4.54, p = 1.9e-2, μ_{L-} = 0.16, μ_{M-} = 0.14, μ_{H-} = 0.15, μ_{L+} = 0.15, μ_{M+} = 0.14, μ_{H+} = 0.17; Figure 18). Under ambient temperature conditions, leaf thickness tends to equally decrease at MWD and HWD, while under warmer temperatures, it tends to increase at HWD. The trees under H+ conditions had significantly thicker leaves than trees under M-, M+, and H- (p = 0.08) conditions.

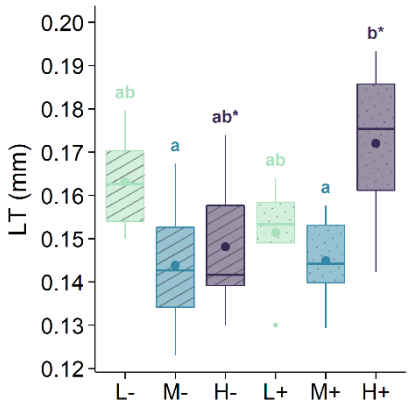

Figure 18. *Q. rubra*'s functional traits that showed a response to water deficit conditional on heat: leaf thickness (LT). Letters denote statistically significant differences between treatments. Similar letters followed by an * indicate that the treatments are equal for an alpha=0.05 while different for an alpha=0.1. Line in the box plots indicates the median values, whereas solid dots indicate the mean values.

Multivariate response to water deficit and heat

None of the axes explain significant trait variation among individuals and treatments (Figure 19). In *Q. rubra*, principal component 1 is significantly correlated with Huber value (r = 0.61, p = 6.13e-5), root mass fraction (r = 0.48, p = 2.88e-3), leaf thickness (r = 0.46, p = 4.72e-3) , intrinsic water use efficiency (r = 0.36, p = 2.87e-2), instantaneous water use efficiency (r = 0.35, p = 3.7e-2), difference in water potentials (r = -0.46, p = 4.7e-3), predawn water potential (r = -0.46, p = 4.23e-8), maximum carbon assimilation per area (r = -0.78, p = 2.53e-8) and per mass (r = -0.80, p = 4.54e-8). All these traits are from the three different organs and are associated with water transport and resource acquisition, conservation, and allocation. Principal component 2 is significantly correlated with intrinsic water use efficiency (r = 0.80, p = 3.08e-9), instantaneous water use efficiency (r = 0.79, p = 1.18e-8), leaf temperature differential (r = 0.58, p = 2.36e-4), predawn water potential (r = 0.43, p = 8.33e-3), root mass fraction (r = 0.4, p = 1.58e-2), and leaf thickness (r = -0.47, p = 4.14e-3). These traits are from the leaf and roots and are associated with water transport, thermoregulation, and resource allocation. Based on the redundancy analysis the water deficit and heat stresses individually and combined explained 10.1% the variation in functional traits values ($F_{(5,30)}$ = 1.79, p = 0.003) with the effect of water deficit (p = 0.005) and heat (p = 0.003) being significant.

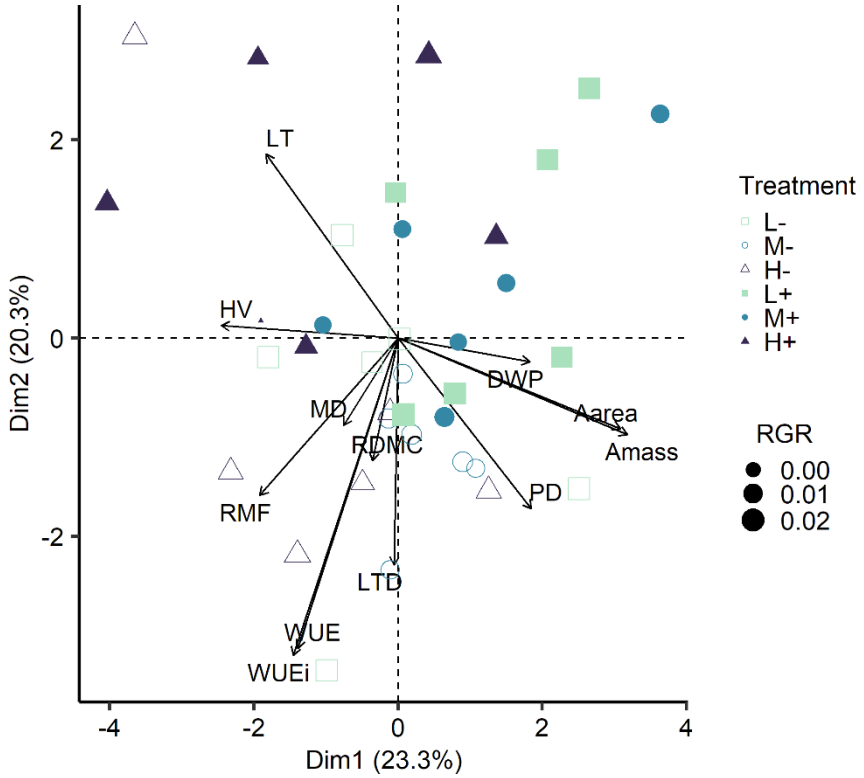

Figure 19. *Q. rubra*'s PCA including all the functional traits that responded to water deficit, heat, and water deficit conditional on heat. Open symbols corresponded to individuals under ambient temperature conditions (without OTC), while solid symbols correspond to individuals under warmer conditions. The green squares correspond to LWD, the blue circles to MWD, and the purple triangles to HWD conditions. The size of the symbols indicates their RGR.

P. glauca

In *P. glauca*, 14 functional traits from the needles and roots showed responses to water deficit and heat stress, with 6 of the 14 traits showing moderate responses of effect sizes between 20 to 47%. Leaf and root traits responded to water deficit conditional on heat (Tables 5 and S1).

Table 5. *P. glauca* summary table of functional traits that responded to the stresses imposed. The parenthesis information indicates the direction of change as a percentage relative to LWD for water deficit, relative to w/o OTC for temperature, and relative to both stresses for the combined treatment.

Stress	Trait
Water deficit	RDMC (+20.4 – 25% HWD)
	LEF (+24.9% MWD)

	LMA (+19.2% HWD)
	RMF (+15.8% HWD)
Heat	LTD (+47.3% OTC)
	g_s (+31.5% OTC)
	E (+30.5% OTC)
	ψ_{MD} (-20.8% OTC)
	CHL (-9.9% OTC)
	WUEi (-9.82% OTC)
	WUE (-8.85% OTC)
Interaction	LT
	SRL
	ARD

Response to Water Deficit

In *P. glauca*, two leaf and two root traits responded to water deficit: leaf mass per area, linear electron flow, root dry matter content, and root mass fraction.

The responses of the two leaf traits to water deficit were not linear. Leaf mass per area values under HWD were similar to those under LWD but were 19.2% higher than under MWD (LMA: $F_{(2,31)}$ = 3.98, p = 2.9e-2, μ_{LWD} = 137, μ_{MWD} = 125, μ_{HWD} = 149; Figure 20A). Linear electron flow, a proxy of photosynthesis, had similar values under LWD and HWD conditions, but showed a marginal increase by 24.9% under MWD compared to LWD (LEF: $F_{(2,27.1)}$ = 2.90, p = 7.2e-2, μ_{LWD} = 22.5, μ_{MWD} = 28.1, μ_{HWD} = 22.8; Figure 20B).

Both root traits increased linearly in response to water deficit. Root dry matter content increase under HWD compared to both LWD and MWD by 25% and 20.4%, respectively (RDMC: $F_{(2,31)}$ = 4.15, p= 2.5e-2, μ_{LWD} = 0.18, μ_{MWD} = 0.19, μ_{HWD} = 0.23; Figure 20C). Finally, root mass fraction showed a marginal response with a 15.8% under HWD compared to LWD (RMF: $F_{(2,31)}$ = 3.04, p= 6.25e-2, μ_{LWD} = *2.97e-1*, μ_{MWD} = 3.02e-1, μ_{HWD} = 3.44e-2; Figure 20D).

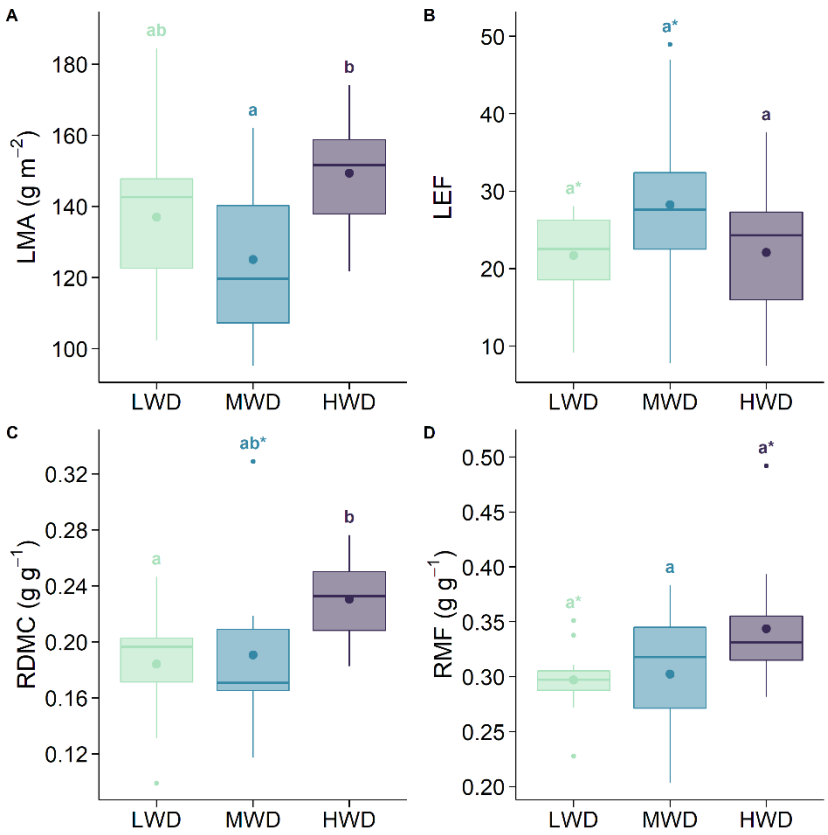

Figure 20. *P. glauca*'s functional traits that responded to water deficit: leaf mass per area (LMA, A), linear electron flow (LEF, B), root dry matter content (RDMC, C), and root mass fraction (RMF, D). Letters denote statistically significant differences between treatments. Similar letters followed by an * indicate that the treatments are equal for an alpha=0.05 while different for an alpha=0.1. Line in the box plots indicates the median values, whereas solid dots indicate the mean values.

Response to Heat

Six leaf traits responded to heat in *P. glauca*: midday water potential, chlorophyll content, stomatal conductance, transpiration, and both instantaneous and intrinsic water use efficiency.

Midday water potential marginally decreased by 20.8% under warmer temperature (ψ_{MD}: $F_{(1,20.1)}$ = 2.97, p= 1.0e-1, $\mu_{w/oOTC}$ = -0.96, μ_{OTC} = -1.16; Figure 21A). Relative chlorophyll concentration decreased by 9.9% under warmer temperature (CHL: $F_{(1,31)}$ = 4.44, p = 4.3e-2, $\mu_{w/oOTC}$ = 546, μ_{OTC} = 492; Figure 21B). Stomatal conductance and transpiration rate increased marginally by 31.5% and 30.5%, respectively, under warmer temperature (g_s: $F_{(1,31)}$ = 3.24, p = 8.1e-2, $\mu_{w/oOTC}$ = 9.18e-2, μ_{OTC} = 1.21e-1. E: $F_{(1,29.9)}$ = 3.19, p = 8.4e-2, $\mu_{w/oOTC}$ = 1.28, μ_{OTC} = 1.67; Figure 21C-D). The instantaneous and intrinsic water use efficiency showed a reduction by 8.85% and 9.82%, respectively, under warmer temperature conditions (WUE: $F_{(1,29.1)}$ = 4.32, p =

4.6e-2, $\mu_{w/oOTC}$ = 7.91, μ_{OTC} = 7.21; WUEi: $F_{(1,31)}$ = 5.62, p = 2.42e-2, $\mu_{w/oOTC}$ = 112, μ_{OTC} = 101; Figure 21E-F).

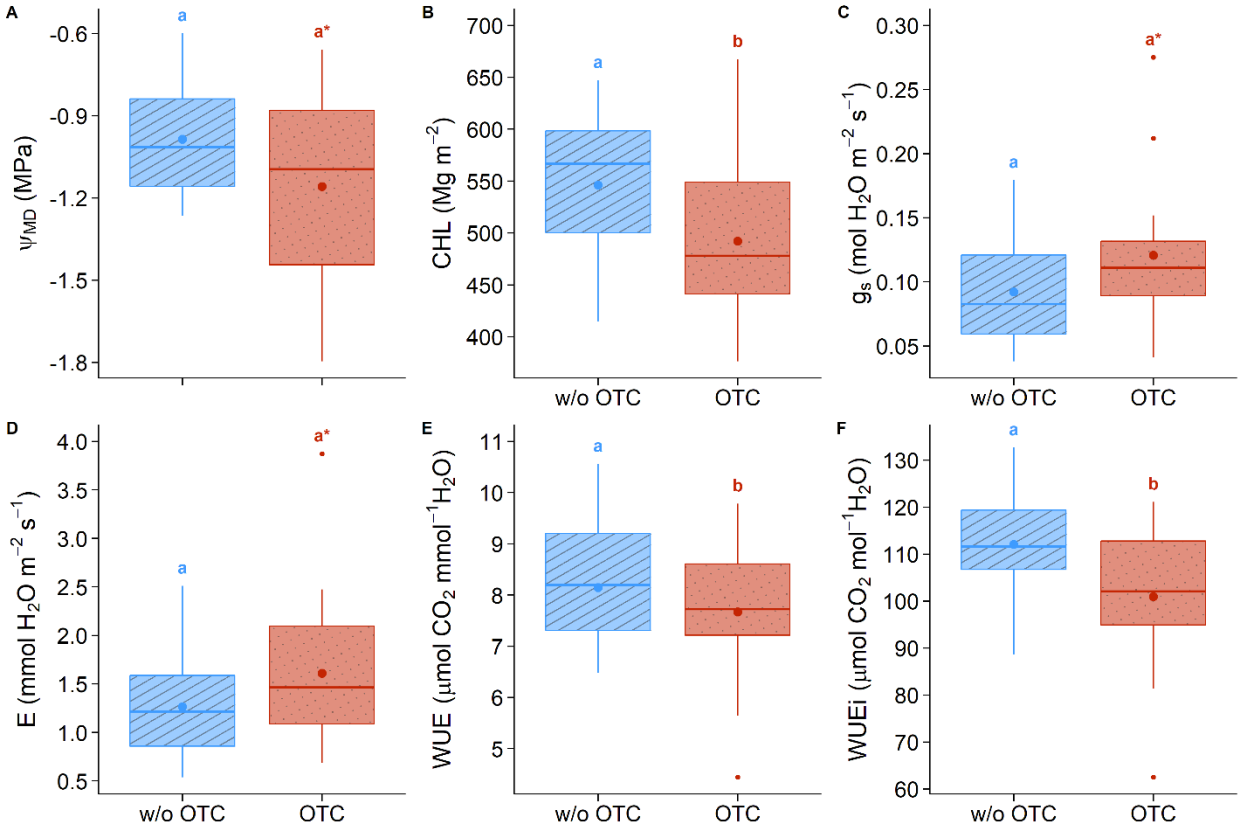

Figure 21. *P. glauca*'s functional traits that responded to heat: midday water potential (ψ_{MD}, A), leaf relative chlorophyll content (CHL, B), stomatal conductance (g_s, C), transpiration rate (E, D), instantaneous water use efficiency (WUE, E), and intrinsic water use efficiency (WUEi, F). Letters denote statistically significant differences between treatments. Similar letters followed by an * indicate that the treatments are equal for an alpha=0.05 while different for an alpha=0.1. Line in the box plots indicates the median values, whereas solid dots indicate the mean values.

Response to Water Deficit conditional on Heat

In *P. glauca*, one leaf trait and two fine-root traits showed different responses to water deficit conditional on heat: needle thickness, specific root length, and root diameter.

Needle thickness showed an opposite response to water deficit depending on heat. Under ambient temperature the needles thickness tends to increase, while under warmer temperatures tends to decrease (LT: $F_{(2,29)}$ = 5.72, p= 8.0e-3, μ_{L-} = 0.51, μ_{M-} = 0.52, μ_{H-} = 0.62, μ_{L-} = 0.59, μ_{M-} = 0.46, μ_{H+} = 0.52, Figure 22A). The needle thickness of both H- and L+ conditions was significantly higher than needle thickness under M+ conditions.

Specific root length and root diameter showed opposite patterns to water deficit depending on heat. Under ambient temperature specific root length showed a decreasing tendency from LWD to HWD but showed the opposite tendency under warmer temperatures with similar values in MWD and HWD conditions (SRL: $F_{(2,29)}$ = 7.06, p = 3.2e-3, μ_{L-} = 67.7, μ_{M-} = 62.9, μ_{H-} = 43.5, μ_{L-} = 36.0, μ_{M-} = 64.8, μ_{H+} = 58.5; Figure 22B). Roots under L+ conditions had significantly lower SRL than roots under M- and M+. The average root diameter showed an increasing tendency from LWD to HWD under ambient temperature but a decreasing tendency from LWD to HWD under warmer temperature (ARD: $F_{(2,29)}$ = 5.62, p = 8.3e-3, μ_{L-} = 0.28, μ_{M-} = 0.32, μ_{H-} = 0.30, μ_{L-} = 0.42, μ_{M-} = 0.32, μ_{H+} = 0.30; Figure 22C). Individuals under L+ conditions had bigger root diameters than individuals under L-, M-, H-, M+, and H+.

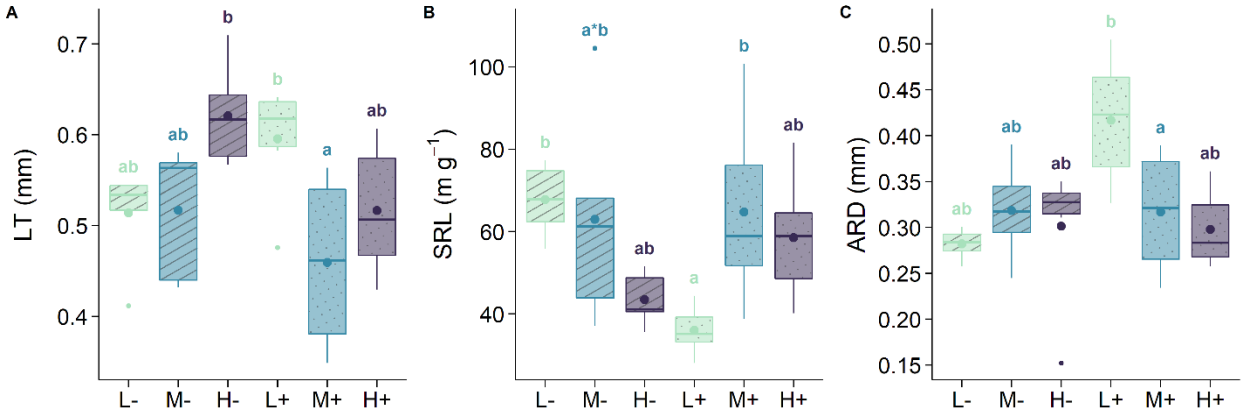

Figure 22. *P. glauca*'s functional traits that showed a response to water deficit conditional on heat: leaf thickness (LT, A), specific root length (SRL, B), and average root diameter (ARD, C). Letters denote statistically significant differences between treatments. Similar letters followed by an * indicate that the treatments are equal for an alpha=0.05 while different for an alpha=0.1. Line in the box plots indicates the median values, whereas solid dots indicate the mean values.

Multivariate response to water deficit and heat

The first axis of variation was significant and explained 27.7% of the variation in functional traits among individuals and treatments (Figure 23). In *P. glauca*, dimension 1 is significantly correlated with transpiration rate (r = 0.94, p = 9.22e-17), stomatal conductance (r = 0.92, p = 8.00e-15), instantaneous water use efficiency (r = -0.84, p = 1.86e-10), intrinsic water use efficiency (r = -0.90, p = 1.09e-13). All these are leaf traits associated with resource acquisition and water use. Dimension 2 is significantly correlated with average root diameter (r = 0.64, p = 3.43e-5), leaf thickness (r = 0.54, p = 7.98e-4), leaf mass per area (r = 0.47, p = 4.15e-3), chlorophyll content (r = 0.38, p = 2.42e-17), leaf temperature differential (r = -0.34, p = 4.85e-2), linear electron flow (r = -0.57, p = 3.85e-4), and specific root length (r = -0.76, p = 1.28e-7). These traits belong to the leaf and roots organs and are associated with water transport and resource acquisition. Based on the redundancy analysis the water deficit and heat stresses individually and combined explained 12.5% of the variation in functional traits values ($F_{(5,29)}$ =

1.98, p = 0.002) with the effect of water deficit (p = 0.023), heat (p = 0.021), and water deficit conditional on heat (p = 0.021) being significant.

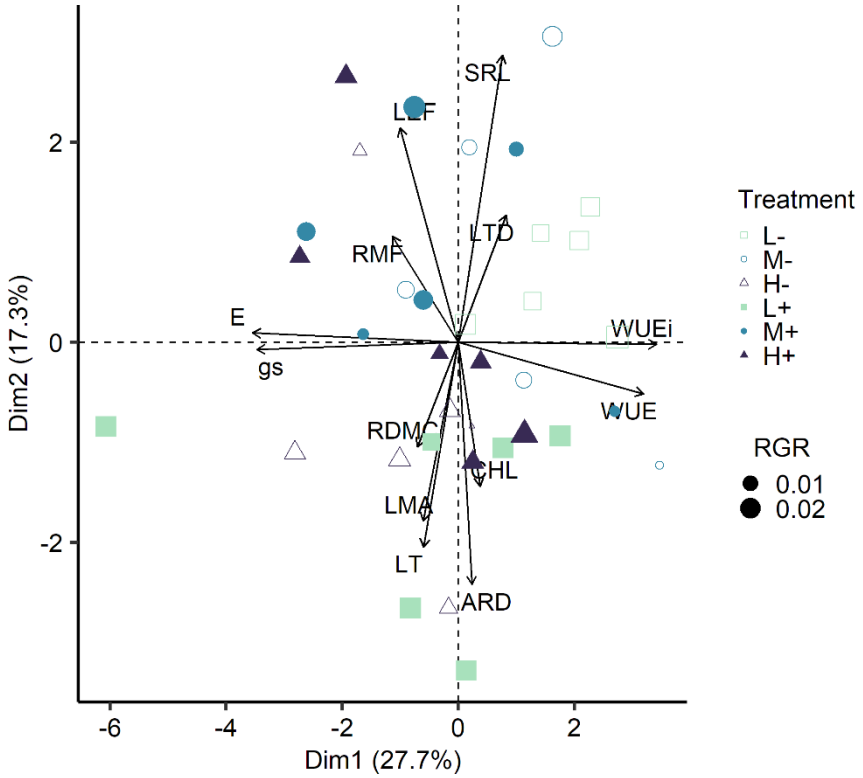

Figure 23. *P. glauca*'s PCA including all the functional traits that responded to water deficit, heat, and water deficit conditional on heat. Open symbols corresponded to individuals under ambient temperature conditions (without OTC), while solid symbols correspond to individuals under warmer conditions. The green squares correspond to LWD, the blue circles to MWD, and the purple triangles to HWD conditions. The size of the symbols indicates their RGR.

P. resinosa

P. resinosa was the species that responded the most to water deficit and heat, with 17 traits from all organs showing a response. Only three leaf traits responded to water deficit. Ten traits from all organs showed a response to heat encompassing multiple physiological functions: temperature regulation, resource acquisition and conservation, mechanical support, and biomass allocation. Four traits from all organs responded to water deficit conditional on heat (Tables 6 and S1).

Table 6. *P. resinosa* summary table of functional traits that responded to the stresses imposed. The parenthesis information indicates the direction of change as a percentage relative to LWD for water deficit, relative to w/o OTC for temperature, and relative to both stresses for the combined treatment.

Stress	Trait
Water deficit	$\Delta\psi$ (+78.7 – 175% MWD)
	ψ_{MD} (+25.8% HWD)
	ψ_{PD} (+22.1 – 23.1% MWD)
Heat	LTD (+56.3 OTC)
	$A_{MAX}{}^{A}$ (-34.4% OTC)
	g_s (-32.9% OTC)
	$A_{MAX}{}^{M}$ (-29.7% OTC)
	E (-26.6% OTC)
	SRL (-16.2% OTC)
	RMF (-12.8% OTC)
	ARD (+12.7% OTC)
	LMF (+3.8 OTC)
	SSD (-3.3% OTC)
Interaction	LT
	LEF
	HV

Response to Water Deficit

In *P. resinosa*, water potential traits showed a non-linear response to water deficit. Predawn water potential was similar between LWD and HWD but had values 22.1 and 23.1% higher under MWD relative to both LWD and HWD (ψ_{PD}: $F_{(2,26.9)}$ = 3.96, p = 3.1e-2, μ_{LWD} = -0.44, μ_{MWD} = -0.34, μ_{HWD} = -0.42; Figure 24A). Midday water potential was 24.6% higher under HWD than MWD (ψ_{MD}: $F_{(2,21.9)}$ = 3.64, p = 4.3e-2, μ_{LWD} = -0.62, μ_{MWD} = -0.73, μ_{HWD} = -0.55; Figure 24B). Together, the shifts in predawn and midday water potentials led to a non-linear change in the water potential difference. Water potential difference was similar between LWD and HWD, and the largest difference was achieved under MWD by increasing in 175% and 78.7% relative to LWD and HWD, respectively (ΔWP: $F_{(2,21.7)}$ = 6.57, p= 5.8e-3, μ_{LWD} = 0.128, μ_{MWD} = 0.351, μ_{HWD} = 0.075; Figure 24C).

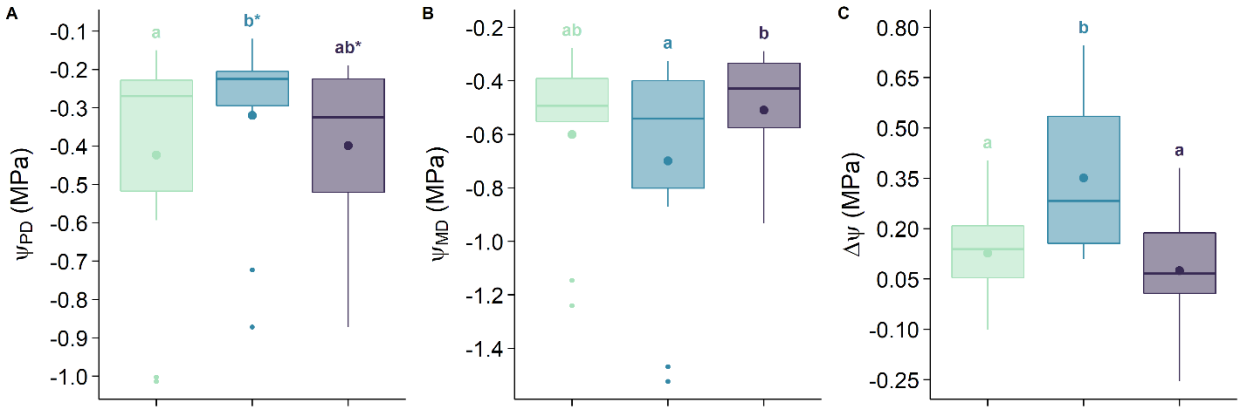

Figure 24. *P. resinosa*'s functional traits that responded to water deficit: predawn water potential (ψ_{PD}, A), midday water potential (ψ_{MD}, B), and the difference between ψ_{PD} and ψ_{MD} ($\Delta\psi$, C). Letters denote statistically significant differences between treatments. Similar letters followed by an * indicate that the treatments are equal for an alpha=0.05 while different for an alpha=0.1. Line in the box plots indicates the median values, whereas solid dots indicate the mean values.

Response to Heat

In *P. resinosa*, nine traits from all organs changed in response to heat: maximum carbon assimilation, stomatal conductance, transpiration rate, specific stem density, specific root length, average root diameter, leaf mass fraction, and root mass fraction.

Maximum carbon assimilation per area and mass decreased by 34.4% and 29.7%, respectively (A_{MAX}^{A}: $F_{(1,30.8)}$ = 8.37, p = 6.9e-3, $\mu_{w/oOTC}$ = 14.41, μ_{OTC} = 9.46; Figure 25A. A_{MAX}^{M}: $F_{(1,29.1)}$ = 4.41, p = 4.4e-*2*, $\mu_{w/oOTC}$ = 128.2, μ_{OTC} = 90.1; Figure 25B). Stomatal conductance and transpiration rate decreased marginally by 32.9% and 26.6% (g_s: $F_{(1,29.6)}$ = 2.79, p = 0.10, $\mu_{w/oOTC}$ = 0.22, μ_{OTC} = 0.15; Figure 25C. E: $F_{(1,29.7)}$ = 3.31, p = 7.9e-2, $\mu_{w/oOTC}$ = 2.9, μ_{OTC} = 2.13; Figure 25D).

Stem specific density decreased by 3.3% under warmer temperatures (SSD: $F_{(1,31)}$ = 8.62, p = 6.2e-3, $\mu_{w/oOTC}$ = 0.571, μ_{OTC} = 0.552; Figure 25E).

Specific root length decreased marginally by 16.2% under warmer temperatures (SRL: $F_{(1,31)}$ = 3.67, p= 6.4e-2, $\mu_{w/oOTC}$ = 50.5, μ_{OTC} = 42.3; Figure 25F), while the average root diameter increased in 12.7% (ARD: $F_{(1,31)}$ = 7.85, p= 8.7e-3, $\mu_{w/oOTC}$ = 0.36, μ_{OTC} = 0.41; Figure 25G).

Leaf mass fraction increased marginally by 3.8% under warmer temperatures (LMF: $F_{(1,31)}$ = 2.92, p = 9.7e-2, $\mu_{w/oOTC}$ = 0.576, μ_{OTC} = 0.598; Figure 25H), while root mass fraction decreased by 12.8% (RMF: $F_{(1,31)}$ = 10.03, p = 3.45e-3, $\mu_{w/oOTC}$ = 0.250, μ_{OTC} = 0.218; Figure 25I).

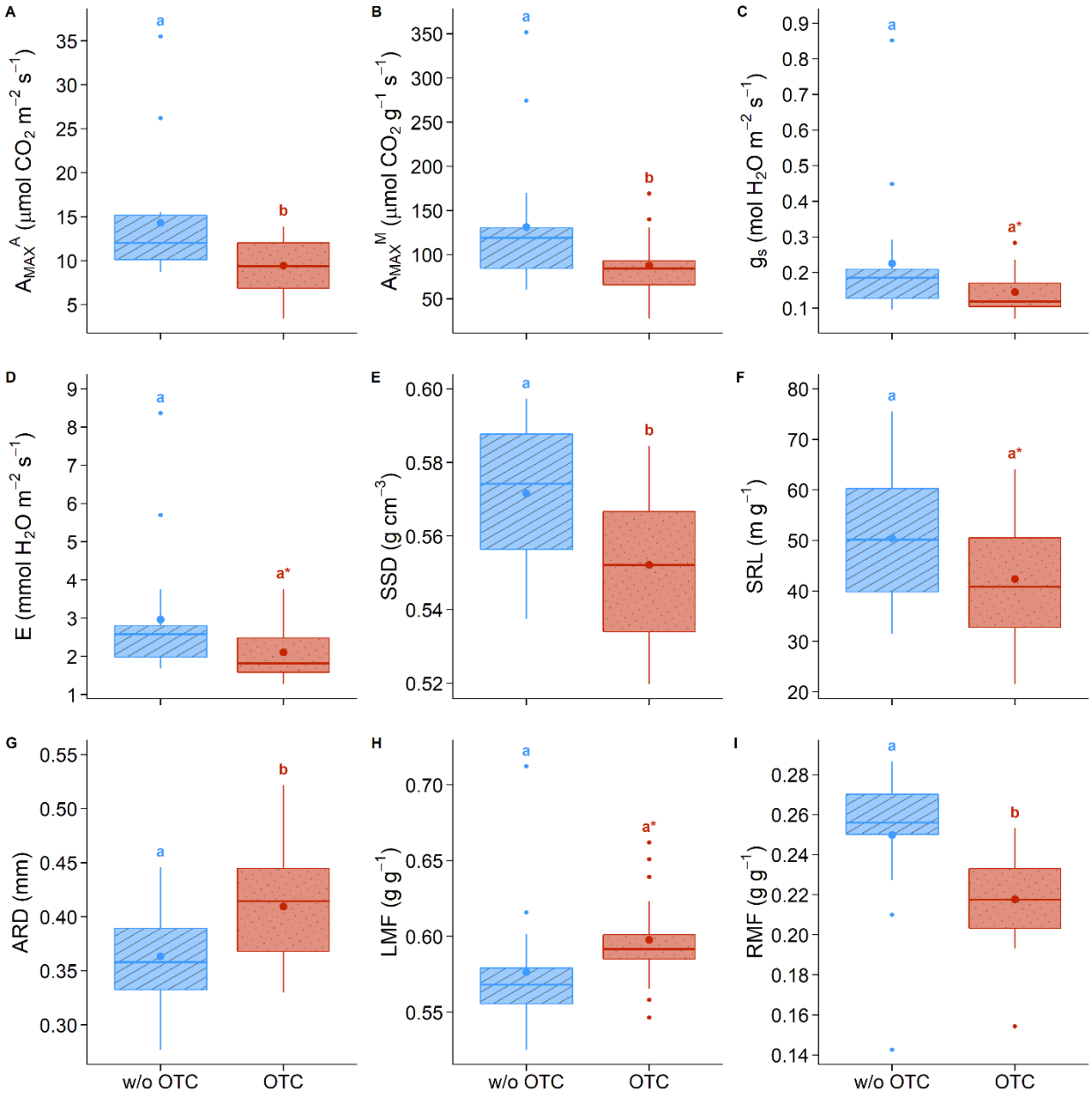

Figure 25. *P. resinosa*'s functional traits that responded to heat: maximum carbon assimilation per area (A_{MAX}^{A}, A), maximum carbon assimilation per mass (A_{MAX}^{M}, B), stomatal conductance (g_s, C), transpiration rate (E, D), stem specific density (SSD, E), specific root length (SRL, F), average root diameter (ARD, G), leaf mass fraction (LMF, H), and root mass fraction (RMF, I). Letters denote statistically significant differences between treatments. Similar letters followed by an * indicate that the treatments are equal for an alpha=0.05 while different for an alpha=0.1. Line in the box plots indicates the median values, whereas solid dots indicate the mean values.

Response to Water Deficit conditional on Heat

P. resinosa's leaf thickness, linear electron flow, Huber value, and root dry matter content showed an interaction in their response to water deficit and heat.

Needles were thinner in MWD under ambient temperature, while their thickness decreased from LWD to HWD under warmer temperatures (LT: $F_{(2,29)}$ = 9.29, p = 7.6e-4, μ_{L-} = 0.53, μ_{M-} = 0.48, μ_{H-} = 0.62, μ_{L+} = 0.63, μ_{M+} = 0.47, μ_{H+} = 0.43; Figure 26A). Trees under both H- and L+ conditions had significantly thicker needles than trees under M-, M+, and H+ conditions.

Linear electron flow, a proxy of photosynthesis, showed a marginal interaction between water deficit and heat (LEF: $F_{(2,24.8)}$ = 3.21, p = 5.8e-2, μ_{L-} = 21.2, μ_{M-} = 23.7, μ_{H-} = 17.4, μ_{L+-} = 16.1, μ_{M+-} = 17.1, μ_{H+} = 19.4; Figure 26B). Under ambient temperature, LEF showed a non-linear tendency with non-significant higher values under MWD, while under warmer temperatures, LEF showed a trend of increasing with water deficit having non-significant higher values under HWD. LEF is marginally higher under M- compared to L+.

The Huber value also showed a marginal interaction between water deficit and heat (HV: $F_{(2,29)}$ = 2.84, p= 7.48e-2, μ_{L-} = 7.40e-4, μ_{M-} = 6.15e-4, μ_{H-} = 5.90e-4, μ_{L+-} = 5.97e-4, μ_{M+-} = 5.54e-4, μ_{H+} = 6.79e-4; Figure 26C). Under ambient temperature, the HV had its highest value under LWD, while under warmer temperature HV is highest under HWD. None of these values are significantly different at alpha=0.05 or 0.1, but under L- conditions, trees had a higher HV than under M+ conditions (p =0.13).

Root dry matter content showed a marginal interaction between water deficit and heat (RDMC: $F_{(2,29)}$ = 2.88, p = 7.25e-2, μ_{L-} = 1.95e-1, μ_{M-} = 2.01e-1, μ_{H-} = 2.06e-1, μ_{L+-} = 1.69e-1, μ_{M+-} = 2.26e-1, μ_{H+} = 1.95e-1; Figure 26D). Under ambient temperature, RDMC has similar values for all levels of water deficit, while under warmer temperatures, roots in MWD and HWD had a higher dry matter content than roots in LWD. Trees under M+ had a higher RDMC than trees under L+ conditions.

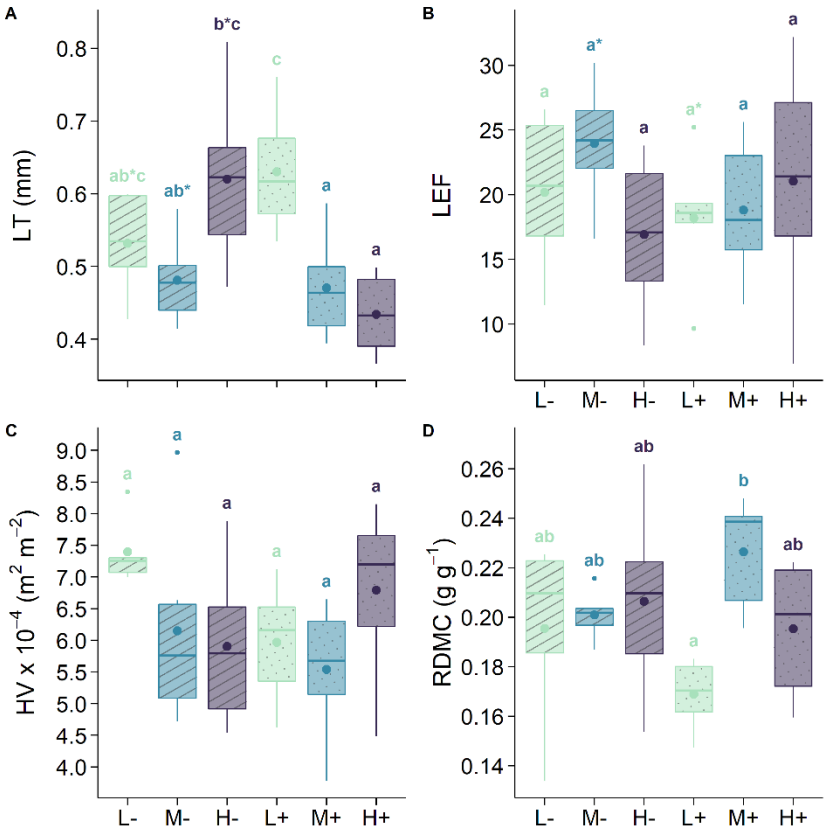

Figure 26. *P. resinosa*'s functional traits that showed a response to water conditional on heat: leaf thickness (LT, A), linear electron flow (LEF, B), Huber values (HV, C), and root dry matter content (RDMC). Letters denote statistically significant differences between treatments. Similar letters followed by an * indicate that the treatments are equal for an alpha=0.05 while different for an alpha=0.1. Line in the box plots indicates the median values, whereas solid dots indicate the mean values.

Multivariate response to water deficit and heat

The fourth first axes of variation were significant and explained 68.1% of the variation in functional traits among individuals and treatments (Figure 23). In *P. glauca*, principal component 1 is significantly correlated with maximum carbon assimilation per area (r = 0.92, p = 4.60e-15), stomatal conductance (r = 0.91, p = 2.09e-14), transpiration rate (r = 0.91, p = 2.18e-14), maximum carbon assimilation per mass (r = 0.9, p = 3.24e-13), root mass fraction (r = 0.4, p = 1.86e-2), leaf mass fraction (r = -0.37, p = 2.91e-02), and average root diameter (r = -0.53, p = 1.17e-3). All these are leaf and root traits associated with resource acquisition, water use, and biomass allocation. Principal component 2 is significantly correlated with average root diameter (r = 0.64, p = 2.58e-5), leaf mass fraction (r = 0.52, p = 1.37e-3), maximum carbon assimilation per mass (r = 0.37, p = 2.79e-2), stem specific density (r = -0.45, p = 7.14e-3), linear electron flow (r = -0.45, p = 5.95e-3), specific root length (r = -0.58, p = 2.25e-4), and root mass fraction (r = -0.64, p = 4.02e-5). These leaf and root traits are associated with resource

acquisition and biomass allocation. Based on the redundancy analysis, water deficit and heat individually and combined explained 12.6% of the variation in functional traits values ($F_{(5,29)}$ = 1.97, p = 0.003), with the effect of heat (p = 0.001) being significant, and the effect of water deficit conditional on heat (p = 0.088) being marginally significant.

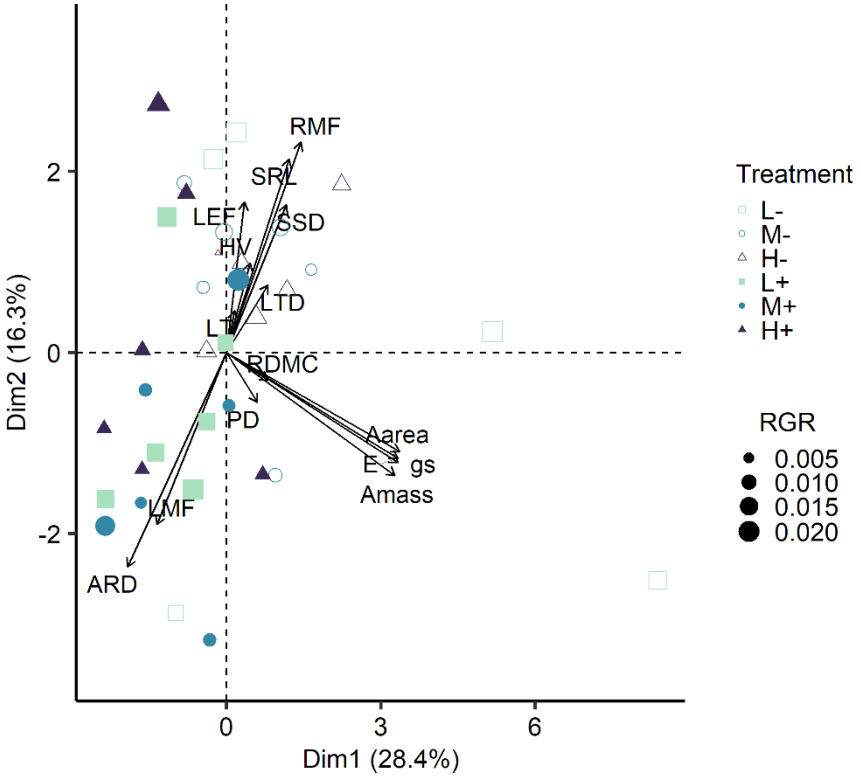

Figure 27. *P. resinosa*'s PCA including all the functional traits that responded to water deficit, heat, and water deficit conditional on heat. Open symbols corresponded to individuals under ambient temperature conditions (without OTC), while solid symbols correspond to individuals under warmer conditions. The green squares correspond to LWD, the blue circles to MWD, and the purple triangles to HWD conditions. The size of the symbols indicates their RGR.

Objective 3 – **Which functional traits mediate trees' performance response (RGR) to water deficit and heat?**

A. saccharum

In *A. saccharum*, change in plant performance (DRGR) was negatively but not significantly correlated with the change in leaf temperature differential (DLTD) and leaf thickness (DLT), and significantly positively correlated with the change in leaf mass per area (DLMA, P<0.05) (Figure 28). The simplified model retained only the change in leaf mass per area that showed a positive linear relationship with the change in relative growth rate ($F_{(1,22)}$ = 4.46, p = 0.046, R^2 = 0.13, Figure 29)

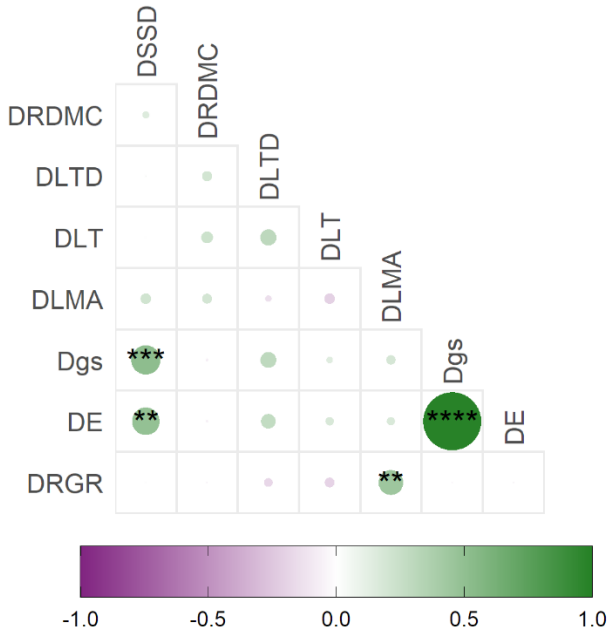

Figure 28. *A. saccharum*'s correlation plot of the change in functional traits and relative growth rate under MWD and HWED. The color and size of the circles indicate the direction and strength of the correlation between variables. Asterisks indicate significant correlations at alpha of 0.1=*, 0.05=**, 0.01=***, and 0.001=****.

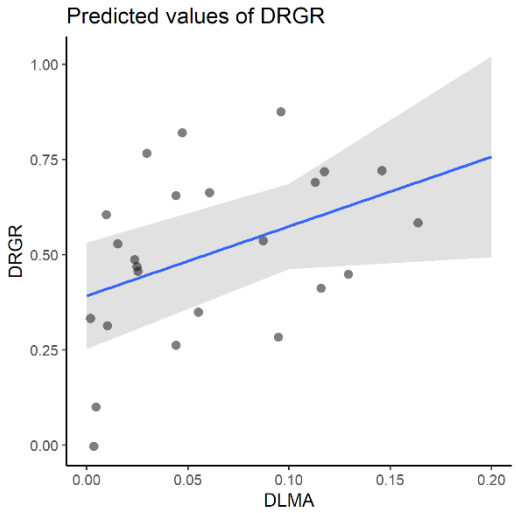

Figure 29. *A. saccharum*'s partial regression plot for the effect of the change in leaf mass per area (DLMA) over the change in relative growth rate (DRGR).

B. alleghaniensis

In *B. alleghaniensis*, change in plant performance (DRGR) was negatively correlated with the change in the amount of light towards non-photochemical quenching (DPhiNPQ, $P<0.1$), and the calculated non-photochemical quenching (DNPQt, $P<0.05$), and non-significantly with the

change in the amount of light towards non-regulated processes (DPhiNO) and root mass fraction (DRMF) (Figure 30). Model selection reveals that none of the changes in traits were linearly associated with the change in relative growth rate, as the simplified model did not retain any

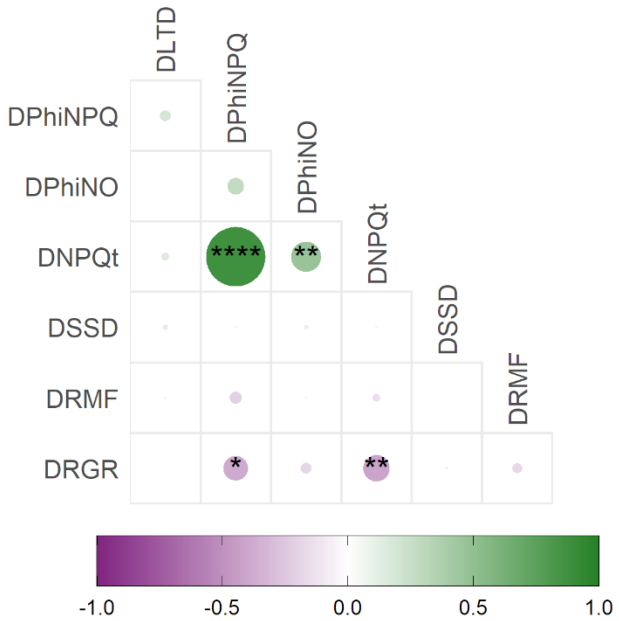

functional trait that showed a response to water deficit and heat individually or combined.

Figure 30. *B. alleghaniensis*'s correlation plot of the change in functional traits and relative growth rate under MWD and HWED. The color and size of the circles indicate the direction and strength of the correlation between variables. Asterisks indicate significant correlations at alpha of 0.1=*, 0.05=**, 0.01=***, and 0.001=****.

Q. rubra

In *Q. rubra*, change in plant performance (DRGR) was negatively correlated with the change in the intrinsic water use efficiency (WUEi, P<0.1) and root dry matter content (DRDMC, P<0.1) and not significantly with the change in predawn leaf water potential (DPD), the difference in the predawn and midday water potential (DWP), the leaf temperature differential (DLTD), and instantaneous water use efficiency (DWUE) (Figure 31). Additionally, it was positively but non-significantly correlated with the change in maximum carbon assimilation per area (DAarea) and per mass (DAmass), and Huber value (DHV) (Figure 31). The significant simplified model retained the change in Huber value and root mass fraction ($F_{(2,21)}$ = 3.56, p = 0.046, R^2 = 0.18, Figure 32C). The change in Huber value effect was marginally significant, showing a positive linear relationship with the change in relative growth rate ($F_{(1,21)}$ = 2.79, p = 0.11, Figure 32A&C). The change in root mass fraction showed a significant negative relationship with the change in relative growth rate ($F_{(1,21)}$ = 4.33, p = 0.049, Figure 32B&C).

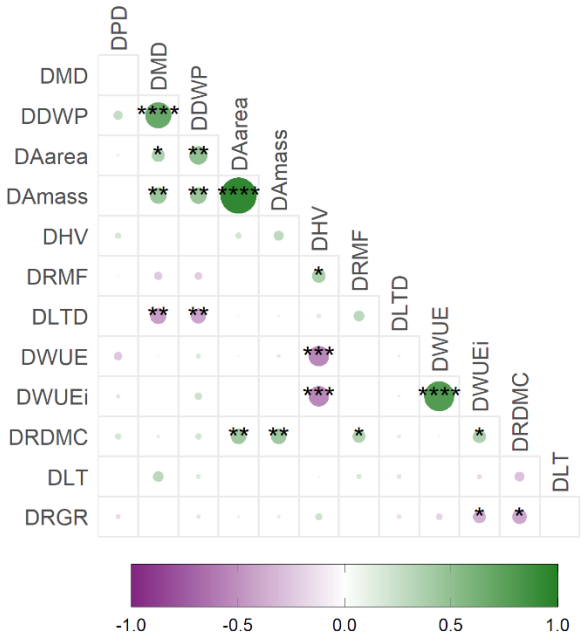

Figure 31. *Q. rubra*'s correlation plot of the change in functional traits and relative growth rate under MWD and HWD. The color and size of the circles indicate the direction and strength of the correlation between variables. Asterisks indicate significant correlations at alpha of 0.1=*, 0.05=**, 0.01=***, and 0.001=****.

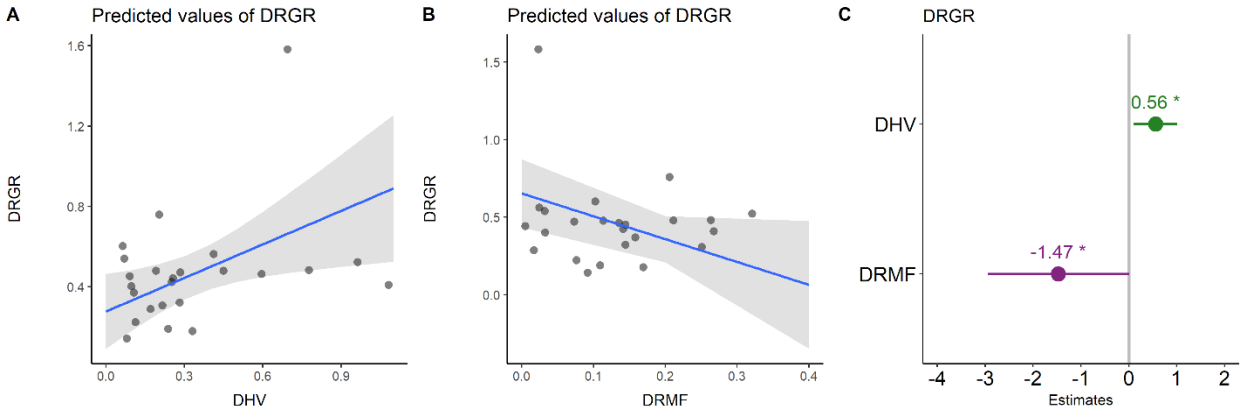

Figure 32. *Q. rubra*'s partial regression plot for the effect of the change in Huber value (DHV, A) and root mass fraction (DRMF, B) over the change in relative growth rate (DRGR) including an effect size plot (C).

P. glauca

In *P. glauca*, change in plant performance (DRGR) was negatively correlated with the change in leaf mass per area (DLMA, P<0.1) and non-significantly with the change in transpiration rate (DE), instantaneous water use efficiency (WUE), midday water potential (DMD), leaf thickness (DLT), and specific root length (DSRL) (Figure 33). Additionally, it was positively but non-

significantly correlated with the change in root dry matter content (DRDMC), root mass fraction (DRMF), leaf temperature differential (DLTD), and chlorophyll content (DCHL) (Figure 33). The significant simplified model retained the change in leaf mass per area, root dry matter content, leaf temperature differential, instantaneous water use efficiency, leaf thickness, and average root diameter ($F_{(6,16)}$ = 5.83, p = 2.2e-3, R^2 = 0.57, Figure 34E). The change in leaf mass fraction showed a significant negative relationship with the change in relative growth rate when considering other functional traits ($F_{(1,16)}$ = 7.32, p = 0.015, Figure 34A&E) and when studied individually ($F_{(1,16)}$ = 3.52, p = 0.074, R^2 = 0.10). The change in leaf temperature differential showed a significant positive relationship with the change in relative growth rate ($F_{(1,16)}$ = 7.12, p = 0.017, Figure 34B&E). The change in instantaneous water use efficiency showed a significant positive relationship with the change in relative growth rate ($F_{(1,16)}$ = 9.84, p = 6.4e-3, Figure 34C&E). The change in average root diameter showed a negative relationship with the change in relative growth rate ($F_{(1,16)}$ = 7.97, p = 0.012, Figure 34D&E). The change in leaf thickness did not have a significant effect on performance when considering other traits but showed a significant negative relationship when alone ($F_{(1,16)}$ = 4.78, p = 0.040, R^2 = 0.15, Data

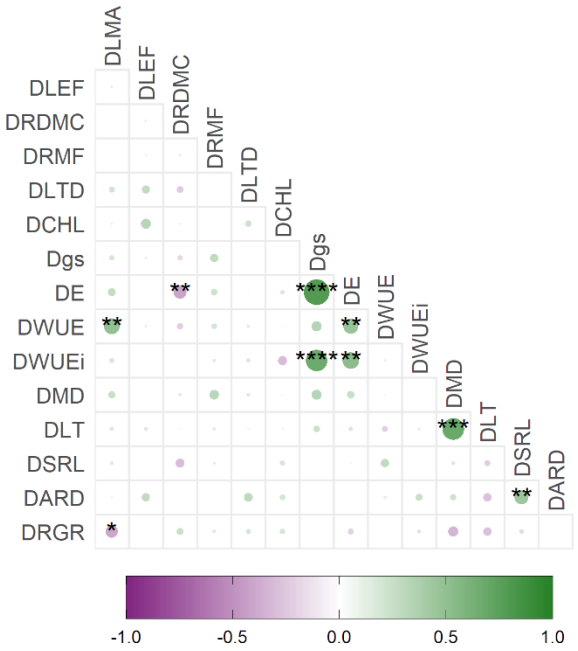

not shown).

Figure 33. *P. glauca*'s correlation plot of the change in functional traits and relative growth rate under MWD and HWED. The color and size of the circles indicate the direction and strength of the correlation between variables. Asterisks indicate significant correlations at alpha of 0.1=*, 0.05=**, 0.01=***, and 0.001=****.

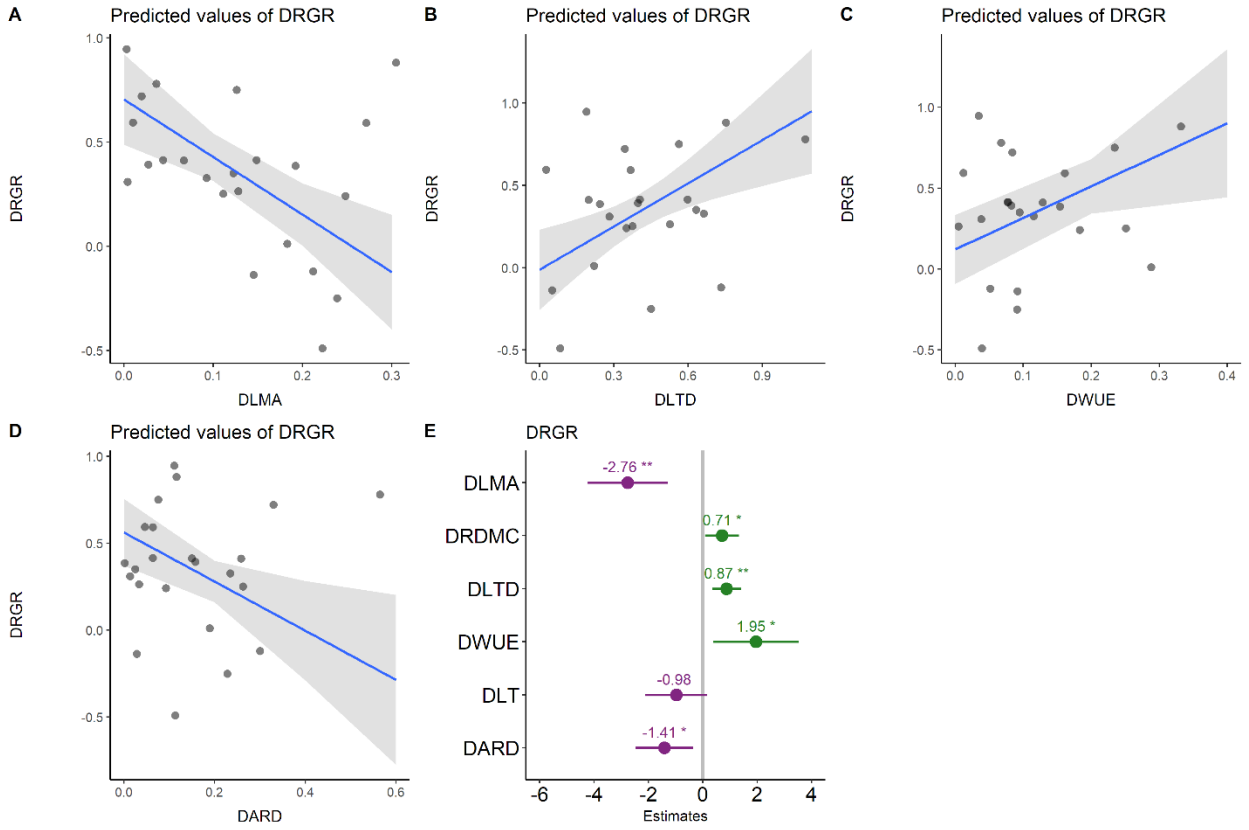

Figure 34. *P. glauca*'s partial regression plot for the effect of the change in leaf mass per area (DLMA, A), leaf temperature differential (DLTD, B), instantaneous water use efficiency (DWUE, C), and overage root diameter (DARD, C) over the change in relative growth rate (DRGR) including an effect size plot with all the variables that were retained in the selected model (E).

P. resinosa

In *P. resinosa*, plant performance (RGR) was negatively but non-significantly correlated with the change in midday water potential (DMD), maximum carbon assimilation per mass (DAmass), average root diameter (DARD), leaf mass fraction (DLMF), and linear electron flow (DLEF) (Figure 35). Additionally, it is positively but non-significantly correlated with the change in predawn water potential (DPD), leaf temperature differential (DLTD), specific root length (DSRL), and Huber Value (DHV) (Figure 35). The significant simplified model retained the change in predawn leaf water potential, leaf temperature differential, maximum carbon assimilation per area and mass, stem specific density, and average root diameter ($F_{(6,17)}$ = 3.30, p = 2.4e-2, R^2 = 0.38, Figure 36D). The change in leaf temperature differential showed a significant positive relationship with the change in relative growth rate ($F_{(1,17)}$ = 4.52, p = 0.049, Figure 36A&D). The change in maximum carbon assimilation per mass showed a marginally significant negative relationship with the change in relative growth rate ($F_{(1,17)}$ = 3.53, p = 0.077,

Figure 36B&D). The change in average root diameter showed a significant negative relationship

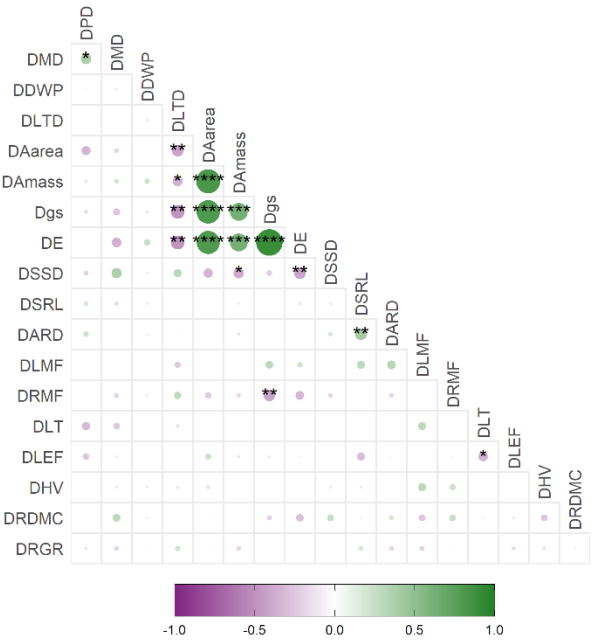

with the change in relative growth rate ($F_{(1,17)}$ = 9.14, p = 7.6e-3, Figure 36C&D).

Figure 35. *P. resinosa*'s correlation plot of the change in functional traits and relative growth rate under MWD and HWED. The color and size of the circles indicate the direction and strength of the correlation between variables. Asterisks indicate significant correlations at alpha of 0.1=*, 0.05=**, 0.01=***, and 0.001=****.

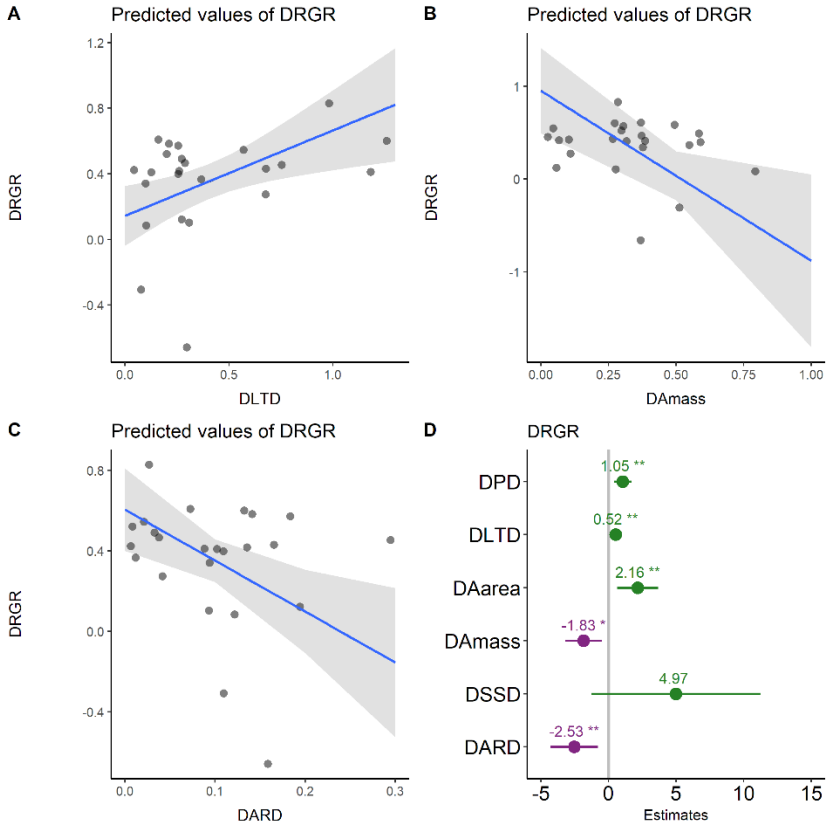

Figure 36. *P. resinosa*'s partial regression coefficient plot for the effect of the change in leaf temperature differential (DLTD, A), maximum carbon assimilation per mass (DAmass, B), and overage root diameter (DARD, C) over the change in relative growth rate (DRGR) including an effect size plot with all the variables that were retained in the selected model (D).

Discussion

Under controlled environmental conditions and limited growing space for roots, we observed that plant performance is reduced with water deficit but not heat, that functional traits from all organs responded more to heat than water deficit, and that a few functional traits per species are correlated with the change in plant performance under water deficit. Moreover, each species showed a unique response because, for each of them, a distinct set of functional traits responded to the stresses imposed.

Objective 1 – RGR decreases with water deficit but not with heat

Increased heat from global warming will affect plant performance in two ways: via a direct effect on plant metabolism and via an indirect effect on water availability. Temperature increase due to global warming without an increase in precipitation will result in drought stress because evaporation will increase, and less water will be available for plants to meet their metabolic

demands via evapotranspiration (Stéfanon et al., 2014). In our experiment, plant performance strongly responded to water deficit for all species, but all species were not detrimentally affected by heat. *P. glauca*, the only species in which RGR responded to heat, showed increased performance under warmer temperatures but decreased with water deficit. If the results from this experiment hold in natural conditions, these patterns suggest that plant performance in many species may decrease with warming via an indirect effect on water availability.

These results may be specific to this experiment, where the warming treatment increased the average daytime temperature in the greenhouse from 25.7°C to 26.2°C and the average nighttime temperature from 22.5°C to 23.1°C. The ambient air temperature was very warm, and the average 0.42°C warming during the day may not have caused any additional stress relative to the ambient air temperature. In an outdoor setting, where airflow maintains lower ambient temperatures most of the summer, warming may reduce RGR (Fisichelli et al., 2012).

Our experimental design of individual open-top chambers exposed plants to an asymmetric increase in temperatures being the nighttime warmer than the daytime. Global climate models highlight that, as the trends have shown, night-time temperatures will keep increasing faster than daytime temperatures (Cox et al., 2020; Desaia et al., 2021). Additionally, Cox et al. (2020) showed that in places where the increase in night-time temperatures has been stronger relative to daytime temperatures, cloud cover, specific humidity, and precipitation increase. Given that in southeastern Canada, we expect similar precipitations with a possible increase of 10%, the effects of global warming could lead to significant differences in nighttime and daytime temperatures. The effects of warmer nights have been broadly studied in crops due to their relevance for food security under future climate conditions (Desaia et al., 2021; Prasad & Djanaguiraman, 2011; Sadok & Jagadish, 2020; Turnbull et al., 2002); however, much uncertainty reaming on the effects of asymmetric temperatures on trees performance and functional traits.

In this study, the trees at ambient temperature were already under heat stress during the daytime, and the addition of open-top chambers did not further increase air temperature during the warmest hours of the day (13h00 – 17h00). Instead, the main effect of the open-top chambers was to retain heat overnight and prevent the trees from fully cooling as ambient temperatures decreased. This heat retention positively affected RGR in *Picea glauca*, a pattern also observed in first-year seedlings exposed in growth chambers to a 3°C increase in temperature (Fisichelli et al., 2014), but not in the field (Fisichelli et al., 2012). This result is unexpected as an increased metabolic rate and nighttime respiration are expected to reduce the amount of carbon available for other metabolic processes, including growth (Sadok & Jagadish, 2020).

Objective 2 – Each species' phenotypic response is unique, and they responded differently to water deficit and heat

Each species showed a unique multivariate response to water deficit and heat individually and combined. Further, each species' response to heat and water deficit was distinct. Despite the widespread consensus that drought and heat should be considered together because of their linkage in Earth's energy and water cycles (Stéfanon et al., 2014), we did not observe a stepper reduction in plant performance under water deficit conditional on heat (M+ and H+). However, more functional traits responded solely to heat on three of the five species (*B. alleghaniensis*, *P. glauca*, and *P. resinosa*).

The only functional trait response shared among all species is an increase in leaf cooling in response to heat. The control of leaf temperature is essential to maximizing carbon assimilation and sustaining plant metabolism under different environmental conditions (Blonder & Michaletz, 2018). Some studies have shown that plants tend to keep their leaf temperature above that of the air in cold and humid environments, while in hot and dry environments, leaf temperature tends to be below air temperature (Blonder & Michaletz, 2018; Deva et al., 2020). Additionally, various authors have found an interaction between genotype and environment (G x E) because warm-adapted genotypes tend to present stronger leaf cooling responses than cold-adapted genotypes (Blasini et al., 2022; Deva et al., 2020; Lin et al., 2017). Moreover, Michaletz et al. (2016) suggested that plant tissue temperature may be included to produce accurate Earth system models, given that leaf thermoregulation contributes to maximizing carbon assimilation across multiple environmental conditions. Our findings that leaf cooling is a common plant response to heat corroborate this recent literature stressing the importance of leaf cooling for plants' response to environmental change.

The treatments imposed in this experiment only increased temperature by an average of 0.42 °C. Nonetheless, the shared response across the five studied species with distinct life histories to this slight increase highlights that controlling leaf temperature is potentially a ubiquitous plant function (Helliker & Richter, 2008). It is worth noting that the stems and foliage of both conifer species studied were wholly covered by the OTCs, while most individuals from the broadleaf species had stems and foliage growing outside of the OTCs. Leaf cooling increased in all species despite these differences in foliage exposure to the warmed air. This suggests that the higher temperatures are not locally sensed by the leaves themselves but are instead detected by the whole plant. Note that the results also suggest that the mechanism by which this shared cooling response was achieved differed among species.

Leaf colling responses observed could be due to heat loss by both convection (i.e., sensible heat), which is mainly controlled by the thickness of the boundary layer, and transpiration (i.e., latent heat), which is mainly controlled by stomata. Only three species showed changes in traits associated with transpiration: two species (*Q. rubra* and *P. glauca*) showed a decrease in their intrinsic water use efficiency (A_{MAX}^{M}/g_s) under warmer temperatures, and *P. glauca* showed an increase (30.5%) in transpiration rate. Thus, the response of *A. saccharum*, *B. alleghaniensis*, and

P. resinosa cannot be directly tied to changes in their transpiration rate, suggesting that sensible heat fluxes are likely to be an essential mechanism for maintaining leaves at optimum functioning temperatures in these species.

In all species except *B. alleghaniesis*, leaf thickness responded to water deficit conditional on heat. The two conifers increased needle thickness when only one of the two stresses is present: under high water deficit at ambient temperature (H-) and low water deficit at high temperatures (L+). This pattern shows that either of the two stresses without the other leads to thicker leaves. In *P. glauca,* the changes in leaf thickness can be associated with changes in leaf mass per area, but not in *P. resinosa*. *P. glauca* showed similar and higher leaf mass per area values under low and high-water deficit relative to medium water deficit associated with a higher leaf thickness in the multivariate space. These different patterns of trait correlation agree with other studies finding that leaf mass per area is strongly related to tissue density or thickness across different environments and in some species (de La Riva et al., 2016; Griffith et al., 2016; Xiong et al., 2016). The two broadleaves, *A. saccharum* and *Q. rubra*, on the other hand, showed different responses. *A. saccharum* had the thickest leaves when both stresses were absent, while *Q. rubra* presented thicker leaves either when both stresses were absent (L-) or present (H+). We interpret these non-linear trait responses to the combination of heat and drought stresses as an indication that the studied species are shifting their response strategies as water deficit becomes stronger or interacts with heat. For example, in *Q. rubra* a mild water deficit at either ambient or warmer temperatures initially led to a change in leaf form (decrease in leaf thickness). However, a high-water deficit with heat instead induced the response of different traits, with the plant shifting to a response in root biomass allocation and water use efficiency instead.

An organism functioning under any environmental conditions relies on numerous traits working simultaneously (Murren, 2002). In this study, we found that three of the five species showed strong trait coordination among traits from different organs and with different putative functional roles: *A.saccharum*, *B. alleghaniensis,* and *P. resinosa*. Trait coordination in different species indicates that patterns of phenotypic integration should be worthy of study under natural conditions. *P. resinosa* showed the strongest phenotypic integration across functional traits from multiple organs. In this specific case, leaf traits associated with the use of water (E) and carbon acquisition (g_s and A_{MAX}^{M}) were highly correlated together and orthogonal to morphological and anatomical traits from the stems and roots (ARD, SRL, SSD), and traits related to biomass allocation (HV, LMF, RMF). Additionally, in *P. resinosa,* trait coordination among root, stem, and biomass allocation traits distinguished the response of plants exposed to ambient temperature to those exposed to warmer temperatures. Therefore, allocation traits may be necessary to understand the individual effects of higher temperatures in natural ecosystems in this species (Freschet et al., 2015; Yin et al., 2019). These results suggest strong species differences in the degree of integration of their plastic response to heat and drought. They also highlight that since water deficit and heat affect different sets of traits, trait coordination on species responses to

changing environmental conditions is worthy of study as it may influence the species' ability to respond to them when combined (Pigliucci, 2003).

Objective 3 – A handful of functional traits contribute to maintain performance under stressful environmental conditions

Only a handful of traits in three of the five species (*P. glauca*, *P. resinosa* and *Q. rubra*) contribute to maintain performance under water deficit conditions. Noteworthy, the two conifers showed the lowest change in relative growth rate under medium water deficit (*P. glauca*: 26.6% and *P. resinosa*: 27.9%), and *Q.* rubra had an intermediate decrease (36.3%) compared to the conifers and other two broadleaves. As evidenced by the decrease in performance, those traits could not compensate for the stressful environmental conditions despite their contribution to maintaining performance.

In *Q. rubra*, an increase by 12% in root mass fraction contributed to maintaining performance, while an increase by 39% in the Huber value had an opposite effect. We expected to observe a generalized increase in the roots mass fraction under water deficit conditions because the optimal partitioning theory suggests that more resources are allocated to the organ that acquires the limiting resource (Bloom, 1985; Luong & Loik, 2022). However, the increase in root biomass allocation was insufficient to offset the effect of a hydraulic safety strategy. A higher Huber value accompanied by lower carbon assimilation and stiffer cell walls resulted in individuals with a lower relative growth rate under high water deficit. A larger HV has been shown to be associated with smaller vessels, higher cavitation resistance, and lower hydraulic efficiency (Markesteijn et al., 2011). Additionally, a reduction in the osmotic potential at full turgor accompanied by stiffer cell walls has been shown to be advantageous under water deficit conditions to prevent cell dehydration and shrinkage (Bartlett et al., 2012). The observed pattern in *Q. rubra* could support the growth-survival trade-off because carbon assimilation is reduced by adopting a hydraulic safety strategy having a substantial impact on yield and, therefore, performance (Meira-Neto et al., 2019; S. J. Wright et al., 2010).

We observed that heat strongly affected functional trait values but not plant performance. Conversely, water deficit significantly affected performance but affected fewer traits than heat. This pattern could be the result of two mechanisms. First, changes in the phenotype might not be correlated with changes in performance. This is unlikely since we measured a comprehensive set of traits, most of which are well documented to vary with environmental gradients ((Pérez-Harguindeguy et al., 2016)).

The second and more possible mechanism is that changes in the phenotype due to warmer temperatures resulted in the maintenance of plant performance. The maintained performance of *P. resinosa* under heat suggests that changes in the phenotype offset the effects of stressful

conditions on plant performance. We found that the maximum carbon assimilation per mass and the average root diameter maintain *P. resinosa*'s performance under water deficit; however, none of these traits responded to water deficit alone. In contrast, the maximum carbon assimilation per mass decreased by 29.7% under warmer temperatures, and the average root diameter increased by 12.7%. Both low maximum carbon assimilation and large root diameters are associated with a conservative resource strategy and drought tolerance (Luong & Loik, 2022).

If these results hold under natural conditions, our study suggests that *A. saccharum* and *B. alleghaniensis* could suffer more than other species under future climate conditions because none of their functional traits that responded to water deficit and heat contributed to mitigate the reduction in relative growth rate. One of the most significant limitations in my ability to infer plant response in natural conditions from this study is that the growing conditions set up in the experiment differ from those in a natural setting. However, this also represents a strength because the experimental design allowed us to assess drought tolerance response by preventing the plants from avoiding water deficit with an increased root foraging. By preventing drought avoidance, we observed that *A. saccharum* and *B. alleghaniensis* experienced the highest reductions in RGR, by 45.6 and 40.6%, respectively, under medium water deficit, with *A. saccharum* having the highest reduction under high water deficit (55.1%) compared to the other three species. In a greenhouse experiment, Hauer et al. (2021) found that ten-week-old seedlings of *A. saccharum* from Ontario sources exposed to water deficit presented an increase in their root to shoot (R:S) ratios and leaf mass per area. Moreover, in this experiment, *A. saccharum* grown under water deficit showed an increase by 22.9% in RDMC, a trait highly correlated with a conservative resource-use strategy (Hogan et al., 2020). Together these results suggest that drought avoidance might be the mechanism available for these two species in natural conditions, especially for *A. saccharum.* Future studies should explore if drought avoidance is the mechanism through investment in high R:S ratios and high root tissue density that allow species to find water while using the available resources moderately (Hauer et al., 2021).

In the three species, two root functional traits contributed to maintaining performance under water deficit conditions. In *Q. rubra*, it was an increase of 12.8% in root mass fraction under high water deficit relative to low. In the two conifers, the average fine-root diameter was increased under warmer temperatures (+12.7% in *P. resinosa*) or under water deficit and ambient temperature (*P. glauca*). As mentioned above, we expected roots to show the most robust plastic responses due to water being the limiting resource (Bloom, 1985; Luong & Loik, 2022). Even though this was not the case, root functional traits mitigate the reduction in relative growth rate under water deficit conditions. In a synthesis of fine-root trait responses to experimental warming, Wang et al. (2021) found that experimental warming resulted in increases in fine-root biomass and nitrogen concentrations and decreases in the carbon-nitrogen ratios; however, it did not affect root morphological traits. Moreover, Wang et al. (2021) did not find an effect of warming on root diameter. Our results, while not wholly aligned with the ones explained above,

could indicate that root diameter should be worthy of study in natural settings for the two conifers studied here.

Conclusion

By exposing seedlings of five tree species from temperate ecosystems to water deficit and heat individually and combined, we found that future warmer and drier conditions will decrease plant performance and impact different species in different ways. The seedlings' performance response was stronger to water deficit than heat, while their plastic trait response was stronger to heat than water deficit. These results highlight that performance and phenotypic responses can be sensitive to different environmental factors. Further, in each species, different traits responded to these two environmental stressors, indicating that the effects of global warming on the phenotype will differ among species. The plastic response to heat and water deficit in all species was distinct. Although heat will lead to water deficit via increased evaporation, results showed that heat and water deficit in all species impact different sets of functional traits. Phenotypic response to global warming sits at the intersection of these two responses, making them more complex to assess. Last, only a total of five traits from three different species contributed to maintain plant performance under water deficit conditions. Still, performance drastically declined in these three species, indicating that plastic responses were insufficient to offset stressful environmental conditions. These complex results highlight the multiple ways global warming will affect species and the many nuances to consider when assessing its effects. This study contributes to trait-based ecology by identifying sets of traits showing plastic responses to warming, which we can use in future studies under controlled and natural conditions to further our knowledge of the effects of global warming on trees.

References

Adams, M. B., Kelly, C., Kabrick, J., & Schuler, J. (2019). *Temperate forests and soils* (pp. 83–108). https://doi.org/10.1016/b978-0-444-63998-1.00006-9

Aitken, S. N., Yeaman, S., Holliday, J. A., Wang, T., & Curtis-McLane, S. (2008). Adaptation, migration or extirpation: climate change outcomes for tree populations. *Evolutionary Applications*, *1*(1), 95–111. https://doi.org/10.1111/j.1752-4571.2007.00013.x

Allen, C. D., Macalady, A. K., Chenchouni, H., Bachelet, D., McDowell, N., Vennetier, M., Kitzberger, T., Rigling, A., Breshears, D. D., Hogg, E. H. (Ted), Gonzalez, P., Fensham, R., Zhang, Z., Castro, J., Demidova, N., Lim, J. H., Allard, G., Running, S. W., Semerci, A., & Cobb, N. (2010). A global overview of drought and heat-induced tree mortality reveals emerging climate change risks for forests. *Forest Ecology and Management*, *259*(4), 660–684. https://doi.org/10.1016/j.foreco.2009.09.001

Bartlett, M. K., Scoffoni, C., & Sack, L. (2012). The determinants of leaf turgor loss point and prediction of drought tolerance of species and biomes: A global meta-analysis. *Ecology Letters*, *15*(5), 393–405. https://doi.org/10.1111/j.1461-0248.2012.01751.x

Bebber, D. P., Holmes, T., & Gurr, S. J. (2014). The global spread of crop pests and pathogens. *Global Ecology and Biogeography*, *23*(12), 1398–1407. https://doi.org/10.1111/geb.12214

Blasini, D. E., Koepke, D. F., Bush, S. E., Allan, G. J., Gehring, C. A., Whitham, T. G., Day, T. A., & Hultine, K. R. (2022). Tradeoffs between leaf cooling and hydraulic safety in a dominant arid land riparian tree species. *Plant Cell and Environment*, *45*(6), 1664–1681. https://doi.org/10.1111/pce.14292

Blonder, B., & Michaletz, S. T. (2018). A model for leaf temperature decoupling from air temperature. *Agricultural and Forest Meteorology*, *262*, 354–360. https://doi.org/10.1016/j.agrformet.2018.07.012

Bloom, A. (1985). Resource Limitation in Plants--An Economic Analogy. *Annual Review of Ecology and Systematics*, *16*(1), 363–392. https://doi.org/10.1146/annurev.ecolsys.16.1.363

Bonamour, S., Chevin, L. M., Charmantier, A., & Teplitsky, C. (2019). Phenotypic plasticity in response to climate change: The importance of cue variation. *Philosophical Transactions of the Royal Society B: Biological Sciences*, *374*(1768). https://doi.org/10.1098/rstb.2018.0178

Bruckman, V. J., & Pumpanen, J. (2019). *Biochar use in global forests: opportunities and challenges* (pp. 427–453). https://doi.org/10.1016/b978-0-444-63998-1.00017-3

Bush, E., & Lemmen, D. S. (Eds.). (2019). *Canada's Changing Climate Report*. Government of Canada. www.ChangingClimate.ca/CCCR2019.

Butterfield, B. J., & Callaway, R. M. (2013). A functional comparative approach to facilitation and its context dependence. *Functional Ecology*, *27*(4), 907–917. https://doi.org/10.1111/1365-2435.12019

Carteron, A., Parasquive, V., Blanchard, F., Guilbeault-Mayers, X., Turner, B. L., Vellend, M., & Laliberté, E. (2019). Soil abiotic and biotic properties constrain the establishment of a dominant temperate tree into boreal forests. *Journal of Ecology*, *108*, 931–944. https://doi.org/10.17504/proto

Chave, J., Coomes, D., Jansen, S., Lewis, S. L., Swenson, N. G., & Zanne, A. E. (2009). Towards a worldwide wood economics spectrum. *Ecology Letters*, *12*(4), 351–366. https://doi.org/10.1111/j.1461-0248.2009.01285.x

Choat, B., Jansen, S., Brodribb, T. J., Cochard, H., Delzon, S., Bhaskar, R., Bucci, S. J., Feild, T. S., & Gleason, S. M. (2012). Global convergence in the vulnerability of forests to drought. *Jordi Martínez-Vilalta*, *11*, 25. https://doi.org/10.1038/nature11688

Chua, S. C., & Potts, M. D. (2018). The role of plant functional traits in understanding forest recovery in wet tropical secondary forests. *Science of the Total Environment*, *642*, 1252–1262. https://doi.org/10.1016/j.scitotenv.2018.05.397

Cohen, S., Bush, E., Zhang, X., Gillett, N., Bonsai, B., Derksen, C., Flato, G., Greenan, B., & E, W. (2019). Synthesis of Findings for Canada's Regions. *Canada's Changing Climate*, 424–443.

Colombo, S. J. (1998). Climatic warming and its effect on bud burst and risk of frost damage to white spruce in Canada. *The Forestry Chronicle*, *74*(4), 567–577.

Cox, D. T. C., Maclean, I. M. D., Gardner, A. S., & Gaston, K. J. (2020). Global variation in diurnal asymmetry in temperature, cloud cover, specific humidity and precipitation and its association with leaf area index. *Change Biol*, *26*, 7099–7111. https://doi.org/10.1111/gcb.15336

Currie, W. S., & Bergen, K. M. (2008). Temperate Forest. In *Encyclopedia of Ecology, Five-Volume Set* (pp. 3494–3503). Elsevier Inc. https://doi.org/10.1016/B978-008045405-4.00704-7

de Frenne, P., de Schrijver, A., Graae, B. J., Gruwez, R., Tack, W., Vandelook, F., Martin, H., & Verheyen, K. (2010). The use of open-top chambers in forests for evaluating warming effects on herbaceous understorey plants. *Ecol. Res.*, *25*, 163–171. https://doi.org/10.1007/s11284-009-0640-3

de Gouvenain, R. C., & Silander, J. A. (2017). Temperate Forests ☆. In *Reference Module in Life Sciences*. Elsevier. https://doi.org/10.1016/b978-0-12-809633-8.02310-4

de La Riva, E. G., Olmo, M., Poorter, H., Ubera, J. L., & Villar, R. (2016). Leaf mass per area (LMA) and its relationship with leaf structure and anatomy in 34 mediterranean woody species along a water availability gradient. *PLoS ONE*, *11*(2). https://doi.org/10.1371/journal.pone.0148788

Desaia, J. S., Lawas, L. M. F., Valentec, A. M., Lemanc, A. R., Grinevicha, D. O., Jagadishb, S. V. K., & Doherty, C. J. (2021). Warm nights disrupt transcriptome rhythms infield-grown rice panicles. *PNAS*, *118*(25), 1–12. https://doi.org/10.1073/pnas.2025899118/-/DCSupplemental

Deva, C. R., Urban, M. O., Challinor, A. J., Falloon, P., Svitákova, L., Fernandez-Aparicio, M., Lee Hatfield, J., Kean Yuen Tan, D., & Morales Sierra, A. (2020). Enhanced Leaf Cooling Is a Pathway to Heat Tolerance in Common Bean. *Article*, *11*, 1. https://doi.org/10.3389/fpls.2020.00019

Djanaguiraman, M., Prasad, P. V. v., & Schapaugh, W. T. (2013). High Day- or Nighttime Temperature Alters Leaf Assimilation, Reproductive Success, and Phosphatidic Acid of Pollen Grain in Soybean [Glycine max (L.) Merr.]. *Crop Science*, *53*, 1594–1604. https://doi.org/10.2135/cropsci2012.07.0441

Dukes, J. S., Jennifer Pontius, David Orwig, Jeffrey, R. G., Vikki, L. R., Nicholas Brazee, Barry Cooke, Kathleen, A. T., Erik, E. S., Robin Harrington, Joan Ehrenfeld, Jessica Gurevitch, Manuel Lerdau, Kristina Stinson, Robert Wick, & Matthew Ayres. (2009). Responses of insect pests, pathogens, and invasive plant species to climate change in the forests of northeastern North America: What can we predict? In *Canadian Journal of Forest Research* (Vol. 39, Issue 2, pp. 231–248). https://doi.org/10.1139/X08-171

FAO. (2020). Global Forest Resources Assessment 2020: Main report. In *Global Forest Resources Assessment 2020*. FAO. https://doi.org/10.4060/ca9825en

Feeley, K. J., Rehm, E. M., & Machovina, B. (2012). The responses of tropical forest species to global climate change: acclimate, adapt, migrate, or go extinct? *Frontiers of Biogeography*, *4*(2). https://doi.org/10.21425/f5fbg12621

Fernández, M. E., & Gyenge, J. E. (2010). *Técnicas en medición en ecofisiología vegetal : conceptos y procedimientos*. INTA.

Fernández, R. J., & Reynolds, J. F. (2000). Potential growth and drought tolerance of eight desert grasses: lack of a trade-off? *Oecologia*, *123*, 90–98. http://jornada.nmsu.edu

Fischer, E. M., & Knutti, R. (2014). Detection of spatially aggregated changes in temperature and precipitation extremes. *Geophysical Research Letters*, *41*(2), 547–554. https://doi.org/10.1002/2013GL058499

Fisichelli, N., Frelich, L. E., & Reich, P. B. (2012). Sapling growth responses to warmer temperatures "cooled" by browse pressure. *Global Change Biology*, *18*(11), 3455–3463. https://doi.org/10.1111/j.1365-2486.2012.02785.x

Fisichelli, N., Wright, A., Rice, K., Mau, A., Buschena, C., & Reich, P. B. (2014). First-year seedlings and climate change: Species-specific responses of 15 North American tree species. *Oikos*, *123*(11), 1331–1340. https://doi.org/10.1111/OIK.01349

Frainer, A., Primicerio, R., Kortsch, S., Aune, M., Dolgov, A. v., Fossheim, M., & Aschan, M. M. (2017). Climate-driven changes in functional biogeography of Arctic marine fish communities. *Proceedings of the National Academy of Sciences of the United States of America*, *114*(46), 12202–12207. https://doi.org/10.1073/pnas.1706080114

Freschet, G. T., Swart Elferra M., & Cornelissen, J. H. C. (2015). Integrated plant phenotypic responses to contrasting above-and below-ground resources: key roles of specific leaf area and root mass fraction. *New Phytologist*, *206*, 1247–1260. https://doi.org/10.1111/nph.13352

Funk, J. L., & Wolf, A. A. (2016). Testing the trait-based community framework: Do functional traits predict competitive outcomes? *Ecology*, *97*(9), 2206–2211. https://doi.org/10.1002/ecy.1484

Gilliam, F. S. (2016). Forest ecosystems of temperate climatic regions: from ancient use to climate change. In *New Phytologist* (Vol. 212, Issue 4, pp. 871–887). Blackwell Publishing Ltd. https://doi.org/10.1111/nph.14255

Gilman, S. E., Urban, M. C., Tewksbury, J., Gilchrist, G. W., & Holt, R. D. (2010). A framework for community interactions under climate change. *Trends in Ecology and Evolution*, *25*(6), 325–331. https://doi.org/10.1016/j.tree.2010.03.002

Goldblum, D., & Rigg, L. S. (2005). Tree growth response to climate change at the deciduous-boreal forest ecotone, Ontario, Canada. *Canadian Journal of Forest Research*, *35*(11), 2709–2718. https://doi.org/10.1139/x05-185

Griffith, D. M., Quigley, K. M., & Anderson, T. M. (2016). Leaf thickness controls variation in leaf mass per area (LMA) among grazing-adapted grasses in Serengeti. *Oecologia*, *181*(4), 1035–1040. https://doi.org/10.1007/s00442-016-3632-3

Hauer, R. J., Wei, H., Koeser, A. K., & Dawson, J. O. (2021). Gas exchange, water use efficiency, and biomass partitioning among geographic sources of acer saccharum subsp. Saccharum and subsp. nigrum seedlings in response to water stress. *Plants*, *10*(4). https://doi.org/10.3390/plants10040742

Heilmeier, H. (2019). Functional traits explaining plant responses to past and future climate changes. In *Flora: Morphology, Distribution, Functional Ecology of Plants* (Vol. 254, pp. 1–11). Elsevier GmbH. https://doi.org/10.1016/j.flora.2019.04.004

Helliker, B. R., & Richter, S. L. (2008). *Subtropical to boreal convergence of tree-leaf temperatures*. *454*. https://doi.org/10.1038/nature07031

Hogan, J. A., Valverde-Barrantes, O. J., Ding, Q., Xu, H., & Baraloto, C. (2020). Morphological variation of fine root systems and leaves in primary and secondary tropical forests of Hainan Island, China. *Annals of Forest Science*, 77–79. https://doi.org/10.1007/s13595-020-00977-7/Published

IPCC. (2014). *Climate change 2014 : Synthesis Report* (R. K. Pachauri & L. A. Meyer, Eds.). IPCC.

Jentsch, A., & Beierkuhnlein, C. (2008). Research frontiers in climate change: Effects of extreme meteorological events on ecosystems. *Comptes Rendus - Geoscience*, *340*(9–10), 621–628. https://doi.org/10.1016/j.crte.2008.07.002

Kelly, A. E., & Goulden, M. L. (2008). Rapid shifts in plant distribution with recent climate change. *Proceedings of the National Academy of Sciences of the United States of America*, *105*(33), 11823–11826. https://doi.org/10.1073/pnas.0802891105

Laliberté, E., Zemunik, G., & Turner, B. L. (2014). Environmental filtering explains variation in plant diversity along resource gradients. *Science*, *345*(6204).

Lambers, H., Chapin, F. S., & Pons, T. L. (2008). Plant physiological ecology: Second edition. In *Plant Physiological Ecology: Second Edition*. Springer New York. https://doi.org/10.1007/978-0-387-78341-3

Lambrecht, S. C., Shattuck, A. K., & Loik, M. E. (2007). Combined drought and episodic freezing effects on seedlings of low- and high-elevation subspecies of sagebrush (Artemisia tridentata). *Physiologia Plantarum*, *130*(2), 207–217. https://doi.org/10.1111/j.1399-3054.2007.00904.x

Laughlin, D. C. (2014). The intrinsic dimensionality of plant traits and its relevance to community assembly. *Journal of Ecology*, *102*(1), 186–193. https://doi.org/10.1111/1365-2745.12187

Lebrija-Trejos, E., Pérez-GarcíA, E. A., Meave, J. A., Bongers, F., & Poorter, L. (2010). Functional traits and environmental filtering drive community assembly in a species-rich tropical system. *Ecology*, *91*(2), 386–398. https://doi.org/10.1890/08-1449.1

Lee, H. K., Lee, S. J., Kim, M. K., & Lee, S. D. (2020). Prediction of plant phenological shift under climate change in south korea. *Sustainability (Switzerland)*, *12*(21), 1–14. https://doi.org/10.3390/su12219276

Leon-Garcia, I. v., & Lasso, E. (2019). High heat tolerance in plants from the Andean highlands: Implications for paramos in a warmer world. *PLOS ONE*, *14*(11), e0224218. https://doi.org/10.1371/journal.pone.0224218

Lin, H., Chen, Y., Zhang, H., Fu, | Peili, Fan, Z., & Watling, J. (2017). Stronger cooling effects of transpiration and leaf physical traits of plants from a hot dry habitat than from a hot wet habitat. *Functional Ecology*, *31*, 2202–2211. https://doi.org/10.1111/1365-2435.12923

Linnakoski, R., Kasanen, R., Dounavi, A., & Forbes, K. M. (2019). Editorial: Forest Health Under Climate Change: Effects on Tree Resilience, and Pest and Pathogen Dynamics. *Frontiers in Plant Science*, *10*, 1157. https://doi.org/10.3389/fpls.2019.01157

Lovett, G. M., Canham, C. D., Arthur, M. A., Weathers, K. C., & Fitzhugh, R. D. (2006). Forest Ecosystem Responses to Exotic Pests and Pathogens in Eastern North America. In *BioScience* (Vol. 56, Issue 5). Oxford Academic. https://doi.org/10.1641/0006-3568(2006)056[0395:FERTEP]2.0.CO;2

Luong, J. C., & Loik, M. E. (2022). Adjustments in physiological and morphological traits suggest drought-induced competitive release of some California plants. *Ecology and Evolution*, *12*(4). https://doi.org/10.1002/ece3.8773

Lynch, A. J., Myers, B. J. E., Chu, C., Eby, L. A., Falke, J. A., Kovach, R. P., Krabbenhoft, T. J., Kwak, T. J., Lyons, J., Paukert, C. P., & Whitney, J. E. (2016). Climate Change Effects on North American Inland Fish Populations and Assemblages. *Fisheries*, *41*(7), 346–361. https://doi.org/10.1080/03632415.2016.1186016

Macgregor, C. J., Thomas, C. D., Roy, D. B., Beaumont, M. A., Bell, J. R., Brereton, T., Bridle, J. R., Dytham, C., Fox, R., Gotthard, K., Hoffmann, A. A., Martin, G., Middlebrook, I., Nylin, S., Platts, P. J., Rasteiro, R., Saccheri, I. J., Villoutreix, R., Wheat, C. W., & Hill, J. K. (2019). Climate-induced phenology shifts linked to range expansions in species with multiple reproductive cycles per year. *Nature Communications*, *10*(1), 1–10. https://doi.org/10.1038/s41467-019-12479-w

Maire, V., Soussana, J. F., Gross, N., Bachelet, B., Pagès, L., Martin, R., Reinhold, T., Wirth, C., & Hill, D. (2013). Plasticity of plant form and function sustains productivity and dominance along environment and competition gradients. A modeling experiment with Gemini. *Ecological Modelling*, *254*, 80–91. https://doi.org/10.1016/j.ecolmodel.2012.03.039

Malhi, Y., Franklin, J., Seddon, N., Solan, M., Turner, M. G., Field, C. B., & Knowlton, N. (2020). Climate change and ecosystems: Threats, opportunities and solutions. *Philosophical Transactions of the Royal Society B: Biological Sciences*, *375*(1794). https://doi.org/10.1098/rstb.2019.0104

Marchin, R. M., Ossola, A., Leishman, M. R., & Ellsworth, D. S. (2020). A Simple Method for Simulating Drought Effects on Plants. *Frontiers in Plant Science*, *10*(1715). https://doi.org/10.3389/fpls.2019.01715

Markesteijn, L., Lourens, P., Horacio, P., Lawren, S., & Frans, B. (2011). Ecological differentiation in xylem cavitation resistance is associated with stem and leaf structural traits Enhanced Reader. *Plant, Cell, and Environment*, *32*, 137–148.

Martin-StPaul, N., Delzon, S., & Cochard, H. (2017). Plant resistance to drought depends on timely stomatal closure. *Ecology Letters*, *20*(11), 1437–1447. https://doi.org/10.1111/ele.12851

Meira-Neto, J. A. A., Nunes Cândido, H. M., Miazaki, Â., Pontara, V., Bueno, M. L., Solar, R., & Gastauer, M. (2019). Drivers of the growth–survival trade-off in a tropical forest. *Journal of Vegetation Science*, *30*(6), 1184–1194. https://doi.org/10.1111/jvs.12810

Michaletz, S. T., Weiser, M. D., McDowell, N. G., Zhou, J., Kaspari, M., Helliker, B. R., & Enquist, B. J. (2016). The energetic and carbon economic origins of leaf thermoregulation. *Nature Plants*, *2*(9). https://doi.org/10.1038/nplants.2016.129

Mouillot, D., Dumay, O., & Tomasini, J. A. (2007). Limiting similarity, niche filtering and functional diversity in coastal lagoon fish communities. *Estuarine, Coastal and Shelf Science*, *71*(3–4), 443–456. https://doi.org/10.1016/j.ecss.2006.08.022

Murren, C. J. (2002). Phenotypic integration in plants. *Plant Species Biology*, *17*, 89–99. https://doi.org/10.1046/j.1441

Pérez-Harguindeguy, N., Días, S., Garnier, E., Lavorel, S., Poorter, H., Jaureguiberry, P., Bret-Harte, M. S., Cornwell, W. K., Craine, J. M., Gurvich, D. E., Urcelay, C., Veneklaas, E. J., Reich, P. B., Porter, L., Wright, I. J., Ray, P., Enrico, L., Pausas, J. C., de Vos, A. C., … Cornelissen, J. H. C. (2016). New handbook for standardised measurement of plant functional traits worldwide. *Australian Journal of Botany*, *64*(8), 715–716. https://doi.org/10.1071/BT12225_CO

Peters, E. B., Wythers, K. R., Zhang, S., Bradford, J. B., & Reich, P. B. (2013). Potential climate change impacts on temperate forest ecosystem processes. *Canadian Journal of Forest Research*, *43*(10), 939–950. https://doi.org/10.1139/cjfr-2013-0013

Pfennig, D. W., & Jane West-Eberhard, M. (Eds.). (2021). *Phenotypic Plasticity & Evolution; Causes, Consequences, Controversies* (First Edition). CRC Press. www.crcpress.com/Evolutionary-

Pigliucci, M. (2003). Phenotypic integration: studying the ecology and evolution of complex phenotypes. *Ecology Letter*, *6*, 265–272. www.genotype-environment.org

Prasad, P. V. V., & Djanaguiraman, M. (2011). High night temperature decreases leaf photosynthesis and pollen function in grain sorghum. *Functional Plant Biology*, *38*(12), 993–1003. https://doi.org/10.1071/FP11035

Rasheed, F., & Delagrange, S. (2016). Acclimation of Betula alleghaniensis Britton to moderate soil water deficit: small morphological changes make for important consequences in crown display. *Tree Physiology*, *36*, 1320–1329. https://doi.org/10.1093/treephys/tpw064

Reich, P. B. (2014). The world-wide "fast-slow" plant economics spectrum: A traits manifesto. *Journal of Ecology*, *102*(2), 275–301. https://doi.org/10.1111/1365-2745.12211

Sadok, W., & Jagadish, S. V. K. (2020). The Hidden Costs of Nighttime Warming on Yields. In *Trends in Plant Science* (Vol. 25, Issue 7, pp. 644–651). Elsevier Ltd. https://doi.org/10.1016/j.tplants.2020.02.003

Snow, M. D., & Tingey, D. T. (1985). Evaluation of a System for the Imposition of Plant Water Stress'. In *Plant Physiol* (Vol. 77). https://plantphysiol.org

Stéfanon, M., Drobinski, P., D'andrea, F., Lebeaupin-Brossier, C., & Bastin, S. (2014). Soil moisture-temperature feedbacks at meso-scale during summer heat waves over Western Europe. *Climate Dynamics*, *42*, 1309–1324. https://doi.org/10.1007/s00382-013-1794-9

Stern, R. L., Schaberg, P. G., Rayback, S. A., Murakami, P. F., Hansen, C. F., & Hawley, G. J. (2020). Growth of canopy red oak near its northern range limit: Current trends, potential drivers, and implications for the future. *Canadian Journal of Forest Research*, *50*(10), 975–988. https://doi.org/10.1139/cjfr-2019-0200

Stige, L. C., & Kvile, K. Ø. (2017). Climate warming drives large-scale changes in ecosystem function. In *Proceedings of the National Academy of Sciences of the United States of America* (Vol. 114, Issue 46, pp. 12100–12102). National Academy of Sciences. https://doi.org/10.1073/pnas.1717090114

Sultan, S. E. (2004). Promising directions in plant phenotypic plasticity. *Perspectives in Plant Ecology,Evolution and Systematics*, *6*(4), 227–233.

Turnbull, M. H., Murthy, R., & Griffin, & K. L. (2002). The relative impacts of daytime and night-time warming on photosynthetic capacity in Populus deltoides. *Plant, Cell and Environment*, *25*, 1729–1737.

Tylianakis, J. M., Didham, R. K., Bascompte, J., & Wardle, D. A. (2008). Global change and species interactions in terrestrial ecosystems. In *Ecology Letters* (Vol. 11, Issue 12, pp. 1351–1363). https://doi.org/10.1111/j.1461-0248.2008.01250.x

van Mantgem, P. J., Stephenson, N. L., Byrne, J. C., Daniels, L. D., Franklin, J. F., Fulé, P. Z., Harmon, M. E., Larson, A. J., Smith, J. M., Taylor, A. H., & Veblen, T. T. (2009). Widespread increase of tree mortality rates in the Western United States. *Science*, *323*(5913), 521–524. https://doi.org/10.1126/science.1165000

Violle, C., Navas, M.-L., Vile, D., Kazakou, E., Fortunel, C., Hummel, I., & Garnier, E. (2007). Let the concept of trait be functional! *Oikos*, *116*(5), 882–892. https://doi.org/10.1111/j.2007.0030-1299.15559.x

Walters, M. B., & Gerlach, J. P. (2013). Intraspecific growth and functional leaf trait responses to natural soil resource gradients for conifer species with contrasting leaf habit. *Tree Physiology*, *33*, 297–310. https://doi.org/10.1093/treephys/tps134

Wang, J., Defrenne, C., Mccormack, M. L., Yang, L., Tian, D., Luo, Y., Hou, E., Yan, T., Li, Z., Bu, W., Chen, Y., & Niu, S. (2021). Fine-root functional trait responses to experimental warming: a global meta-analysis. *New Phytologist*, *230*, 1856–1867. https://doi.org/10.1111/nph.17279

Weemstra, M., Mommer, L., Visser, E. J. W., van Ruijven, J., Kuyper, T. W., Mohren, G. M. J., & Sterck, F. J. (2016). Towards a multidimensional root trait framework: a tree root review. In *The New phytologist* (Vol. 211, Issue 4, pp. 1159–1169). Blackwell Publishing Ltd. https://doi.org/10.1111/nph.14003

Welshofer, K. B., Zarnetske, P. L., Lany, N. K., & Thompson, L. A. E. (2017). *Open-top chambers for temperature manipulation in taller-stature plant communities*. https://doi.org/10.1111/2041-210X.12863

Williams, L. E., & Araujo, F. J. (2002). Correlations among predawn leaf, midday leaf, and midday stem water potential and their correlations with other measures of soil and plant water status in Vitis vinifera. *Journal of the American Society for Horticultural Science*, *127*(3), 448–454. https://doi.org/10.21273/jashs.127.3.448

Wilson, J. B., & Stubbs, W. J. (2012). Evidence for assembly rules: Limiting similarity within a saltmarsh. *Journal of Ecology*, *100*(1), 210–221. https://doi.org/10.1111/j.1365-2745.2011.01891.x

Wright, I. J., Reich, P. B., Westoby, M., Ackerly, D. D., Baruch, Z., Bongers, F., Cavender-Bares, J., Chapin, T., Cornellssen, J. H. C., Diemer, M., Flexas, J., Garnier, E., Groom, P. K., Gulias, J., Hikosaka, K., Lamont, B. B., Lee, T., Lee, W., Lusk, C., … Villar, R. (2004). The worldwide leaf economics spectrum. *Nature*, *428*(6985), 821–827. https://doi.org/10.1038/nature02403

Wright, S. J., Kitajima, K., Kraft, N. J. B., Reich, P. B., Wright, I. J., Bunker, D. E., Condit, R., Dalling, J. W., Davies, S. J., Díaz, S., Di´az, D., Engelbrecht, B. M. J., Harms, K. E., Hubbell, S. P., Marks, C. O., Ruiz-Jaen, M. C., Salvador, C. M., & Zanne, A. E. (2010). Functional traits and the growth-mortality trade-off in tropical trees. In *Ecology* (Vol. 91, Issue 12).

Xiong, D., Wang, D., Liu, X., Peng, S., Huang, J., & Li, Y. (2016). Leaf density explains variation in leaf mass per area in rice between cultivars and nitrogen treatments. *Annals of Botany*, *117*(6), 963–971. https://doi.org/10.1093/aob/mcw022

Xu, J., Chai, Y., Wang, M., Dang, H., Guo, Y., Chen, Y., Zhang, C., Li, T., Zhang, L., & Yue, M. (2018). Shifts in Plant Community Assembly Processes across Growth Forms along a Habitat Severity Gradient: A Test of the Plant Functional Trait Approach. *Frontiers in Plant Science*, *9*, 180. https://doi.org/10.3389/fpls.2018.00180

Yin, Q., Tian, T., Han, X., Xu, J., Chai, Y., Mo, J., Lei, M., Wang, L., & Yue, M. (2019). The relationships between biomass allocation and plant functional trait. *Ecological Indicators*, *102*, 302–308. https://doi.org/10.1016/j.ecolind.2019.02.047

Zhang, X., Flato, G., Kirchmeier-Young, M., Vincent, L., Wan, H., Wang, X., Rong, R., Fyfe, J., Li, G., & Kharin, V. V. (2019). Changes in Temperature and Precipitation Across Canada. In E. Bush & D. S. Lemmen (Eds.), *Canada's Changing Climate Report. Government of Canada* (pp. 112–193).

Zuur, A. F., & Ieno, E. N. (2016). A protocol for conducting and presenting results of regression-type analyses. *Methods in Ecology and Evolution*, *7*(6), 636–645. https://doi.org/10.1111/2041-210X.12577

Zuur, A. F., Ieno, E. N., & Elphick, C. S. (2010). A protocol for data exploration to avoid common statistical problems. *Methods in Ecology and Evolution*, *1*(1), 3–14. https://doi.org/10.1111/j.2041-210x.2009.00001.x